

# DEEP INELASTIC ELECTRON AND MUON SCATTERING

R. E. Taylor

Stanford Linear Accelerator Center, Stanford University, Stanford, California, USA.

## INTRODUCTION

Last summer there was great concern over an apparent contradiction between storage ring data on hadron production<sup>1,2)</sup> and theoretical predictions based on scaling in deep inelastic scattering experiments.<sup>3,4)</sup> Last fall, along with the discovery of the new particles,<sup>5,6)</sup> more accurate data on the ratio

$$R_A = \frac{\sigma_{\text{tot}}(e^+e^- \rightarrow \text{hadrons})}{\sigma_{\text{tot}}(e^+e^- \rightarrow \mu^+\mu^-)} \quad (1)$$

became available<sup>7)</sup> (Fig. 1). At low values of  $E_{\text{cm}}$ ,  $R_A$  now appears to be compatible with a constant as expected, and the value of  $R_A$  in this region is not too far from a model prediction based on colored quarks in which  $R_A = 2$ . The existence of the new particles provides a rationale for the step in  $R_A$  between  $E_{\text{cm}} = 3.5$  GeV and  $E_{\text{cm}} = 5$  GeV so the conflict between these data and deep inelastic scattering has been removed, at least for the present.

The new particles and the step in  $R_A$  may, however, have effects in the deep inelastic. In 1973, at Bonn, Bjorken<sup>8)</sup> drew several pictures interpreting the large values of  $R_A$  from CEA in different ways. Figure 2 shows one of these pictures, and Figure 3 is an update of another figure in his talk, indicating that there may be enhancements of the structure functions above the color or charm thresholds. Obviously, Figure 3 is just a qualitative guess, but the discovery of a new mass scale some three times heavier than the proton introduces yet another way in which scaling in the deep inelastic region may be broken. In addition, the  $\psi$  mesons are vector mesons and will be diffractively produced like  $\rho$  mesons. In inclusive scattering experiments the low mass vector mesons may be important at small  $x$ , and similar effects due to the  $\psi$  mesons might be seen if  $Q^2 > M_\psi^2$ . Even though  $\psi$  production effects may be small in inclusive measurements, electroproduction of  $\psi$ 's should occur, although they have not been detected to date. The Chicago-Harvard-Illinois-Oxford collaboration at NAL have searched their  $\mu$  scattering data tapes for  $\mu$  tridents arising from  $\mu$  pair decay of  $\psi$ 's, but their sensitivity is limited, and none were found.<sup>9,23b)</sup> They are improving the sensitivity of the apparatus to such events for future runs. In an abstract submitted to this conference, the Cornell-Michigan State-Princeton-San Diego group<sup>10,23a)</sup> report the observation of muon tridents in their apparatus at NAL. They will present results to the conference.

The effect of the two  $\psi$ 's on the elastic form factors is expected to be very small,  $< 10^{-3}$  even at  $Q^2 = 30 \text{ (GeV/c)}^2$  basically because the coupling of the  $\psi$ 's to hadrons is so weak. The  $E_{\text{cm}} = 4.2$  GeV "disturbance" has a larger width and might give a larger contribution, but its properties are not yet well established.

A more speculative possibility concerns the existence of other new particles, related to the  $\psi$ 's. If there existed charged particles (positive charge, and baryon number = 1) they could show up as peaks in inelastic scattering spectra. (In addition, pair or associated production of particles should cause a "step" in the spectrum at the appropriate threshold, but since  $\pi$ 's,  $K$ 's,  $K\Lambda$ , etc., are not detected in this way, this is not a very sensitive way to hunt for new particles.) In a previous (Invited paper presented at the Int. Conf. on High Energy Physics sponsored by the European Physical Society, Palermo, Italy, June 23-28, 1975.)

experiment, SLAC (Group A)<sup>11)</sup> had made a high resolution study of inelastic spectra at  $4^\circ$  up to final state masses of 3 GeV. After the announcement of the new particles, we completed these "scans" to the limits set by SLAC's beam energy. No spikes (or steps) were seen (Fig. 4). Roughly speaking, anything with an amplitude of about 10% of the third resonance, and a width less than a few hundred MeV, would have been visible. For resonances of widths smaller than the experimental resolution ( $\sim 5$  MeV) such a criterion corresponds very roughly speaking to an integrated total photo cross section of  $\lesssim 8 \mu\text{b-MeV}$ .

So, for now, the major consequence of the new discoveries for deep inelastic scattering is the rehabilitation of the constituent models which grew out of Bjorken's early predictions<sup>12)</sup> and the deep inelastic scattering data. We, therefore, return to the problem of measuring the nucleon structure functions where the principal topic of interest is still the status of scaling of the structure functions. This topic was carefully reviewed by Gilman at London in 1974.<sup>4)</sup>

### ELASTIC SCATTERING

Before covering the progress since London on that topic, I want to comment on some elastic electron scattering results. Figure 5 shows  $Q^4 G_M^P$  plotted against  $Q^2$ . There are some new measurements<sup>13)</sup> shown, including a point at  $Q^2 = 33(\text{GeV}/c)^2$ , but the main point I want to make is the convincing evidence for  $1/Q^4$  behavior at large  $Q^2$ . Brodsky and Farrar<sup>14)</sup> have pointed out a connection between the power behavior of  $G_M^P$  and the number of "fields" in the hadron under their dimensional scaling laws. For the observed  $1/Q^4$  behavior this gives three fields for the proton. West<sup>15)</sup> has pointed out (with his tongue at least partly in his cheek) that the lack of diffraction in the elastic form factor is some kind of evidence against a large number of constituents. More generally the obvious difference in  $Q^2$  behavior in elastic and inelastic scattering is in itself significant (though not conclusive) evidence for nucleon substructure.

Figure 6 shows some recent results from a coincidence experiment measuring elastic e-d scattering by Arnold et al.<sup>16)</sup> The cross section drops precipitously and shows no sign of flattening out, as might have been expected for scattering from meson exchange currents. The data are in rough agreement with some of the standard fits to lower  $Q^2$  data and possibly approach the  $Q^{-20}$  dependence which can be obtained from simple quark counting.

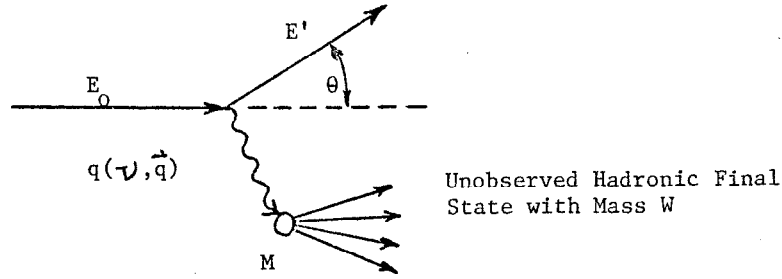
### INELASTIC STRUCTURE FUNCTIONS

In the one photon approximation, inclusive electron scattering cross sections from unpolarized nucleons can be expressed as

$$\frac{d\sigma}{d\Omega dE'} = \left(\frac{d\sigma}{d\Omega}\right)_{\text{Mott}} \left\{ W_2(\nu, Q^2) + 2 \tan^2 \theta/2 W_1(\nu, Q^2) \right\} \quad (2)$$

$$\left(\frac{d\sigma}{d\Omega}\right)_{\text{Mott}} = \frac{\alpha^2 \cos^2 \theta/2}{4E_0^2 \sin^4 \theta/2}$$

$$-q^2 = Q^2 = 4E_0 E' \sin^2 \theta/2, \quad \nu = E_0 - E', \quad W^2 = 2M\nu + M^2 - Q^2 \quad (3)$$



$$\omega = \frac{2M\nu}{Q^2}, \quad \omega' = \frac{W^2}{Q^2} + 1 = \omega + \frac{M^2}{Q^2} \quad (4)$$

$$W_1 = \frac{K}{M^2} \frac{\sigma_T}{\sigma_0}, \quad W_2 = \frac{K}{M^2} \frac{Q^2}{Q^2 + \nu^2} \frac{\sigma_T + \sigma_S}{\sigma_0} \quad (5)$$

$$\sigma_0 = \frac{4\pi^2\alpha}{M^2} = 127 \mu b, \quad R = \frac{\sigma_S}{\sigma_T}, \quad K = \frac{W^2 - M^2}{2M} \quad (6)$$

Ideally, one wishes to obtain  $W_1$  and  $W_2$  from measurements of differential cross sections and test the resulting structure functions for scaling.<sup>12)</sup>

$$Q^2 \lim_{Q^2 \rightarrow \infty} \nu W_2(\nu, Q^2) = F_2(\omega), \quad Q^2 \lim_{Q^2 \rightarrow \infty} 2MW_1(\nu, Q^2) = F_1(\omega) \quad (7)$$

Definition of a kinematic region in which scaling is expected to hold is not a trivial task. Fig. 7 shows some of the problems which occur:

- 1) Two-photon Exchange. The usual analysis neglects two-photon exchange effects. If such effects are present, the measured values of  $\nu W_2$  and  $W_1$  obtained from experiment will be incorrect. Such terms should show up first at high  $Q^2$  and low  $W$  where the cross sections are smallest.
- 2)  $Q^2$  Turn On.  $W_2 = 0$  at  $Q^2 = 0$ , so  $\nu W_2$  will not scale for low  $Q^2$ . This region is further complicated by diffractive processes (e.g., vector meson production).
- 3) Resonance Region. The structure functions will not scale in a region where resonances occur at fixed values of  $W$  and therefore different values of  $\nu/Q^2$ . Strong assumptions about local duality have been used to connect average values of  $\nu W_2$  from these regions to values at higher  $Q^2$ .<sup>17)</sup>
- 4) Non Leading Terms. In the region of finite  $Q^2$  the structure functions may contain terms with powers of  $1/Q^2$  which can produce measurable effects. Such terms may be more important at low  $\omega$  where the cross sections are small.
- 5) Choice of Scaling Variable. The scaling variable,  $\omega$ , can in principle be replaced by any variable which approaches  $\omega$  in the limit  $Q^2 \rightarrow \infty$ .  $\omega$  is an appealing variable because elastic scattering from light, free constituents would give a peak at  $\omega = M/M_c$ , where  $M_c$  is the mass of the constituent.
- 6) Scale Breaking. Various ways in which the scaling conjecture might be modified have been proposed. Popular examples of scale breaking are:

color or charm "thaw";<sup>13)</sup>  
 parton form factors,<sup>19)</sup> anomalous moments;<sup>20)</sup>  
 theories with anomalous dimensions;<sup>21)</sup> and  
 asymptotically free theories.<sup>22)</sup>

The experimentalists' aim is to establish scaling in some region (and to some accuracy), and then look for various scale breaking phenomena such as those listed under No. 6. It is difficult to reach definite conclusions when the observation of apparent non-scaling behavior may be due to one or more of the other effects listed above. There are both old and new examples of this problem. As the range and precision of the data increase, we need a corresponding increase in theoretical understanding and precision to deal with effects at finite  $Q^2$ .

### ELECTRON SCATTERING

The past two years have seen considerable growth in the amount of experimental data, including the first results on really deep inelastic scattering using both neutrinos<sup>4)</sup> and  $\mu$  mesons<sup>23)</sup> from the Fermilab accelerator. Figure 8 shows the kinematic range available in the  $Q^2, W^2$  plane for SLAC energies and for 56 and 150 GeV  $\mu$  mesons, the latter two energies being those of the "scale invariant"  $\mu$  experiment at NAL. That Bjorken's predictions have withstood the strain of increasing  $\nu$  by almost an order of magnitude is truly impressive, as is the spectacular agreement of the neutrino experiments with the simple quark ideas. Meanwhile, back at the Farm, electron scattering experiments have continued, increasing both the precision and kinematic range compared with earlier experiments at SLAC. Data taking has recently begun on an experiment using polarized electrons and a polarized target, but no results are available yet.<sup>24)</sup>

The structure functions  $W_1$  and  $W_2$  can be determined from measurements of the differential cross section. Figure 9 shows the region in which measurements can be made for energies employed at SLAC and in the Cornell-Michigan State-Princeton apparatus at NAL.<sup>25)</sup> Values for each of the structure functions can only be obtained by doing measurements at various angles for a given  $Q^2$  and  $W$ . If measurements exist at only one angle, some assumption must be made about the relationship between  $W_1$  and  $W_2$  to obtain the value of either structure function. The relationship is usually described in terms of the longitudinal/transverse ratio  $R = \sigma_S/\sigma_T$  (see Eq. (6)). For some kinematics, the structure functions are not very sensitive to  $R$ . For example, we can write

$$\nu W_2 = \frac{\sigma_{\text{Meas}}}{\sigma_{\text{Mott}}} \left[ 1 + \frac{(1 + \nu^2/Q^2)}{(1+R)} 2 \tan^2 \theta/2 \right]^{-1} \quad (8)$$

If  $\theta$  is small enough, then the second term may be quite unimportant. The region where  $\nu W_2$  varies less than 10% as  $R$  varies from 0 -  $\infty$  is shown in Fig. 2 (for 20 GeV incident energy this region is smaller than the region in which measurements of  $R$  have been made). If  $0 < R < 1$ , the maximum error in the indicated region would drop to 5%. Figure 10 shows in more detail the regions in which  $W_1$  and  $W_2$  have been separated to date.

The most recent published results on  $W_1$  and  $W_2$  are those of the MIT-SLAC (SFG Group).<sup>26)</sup> Using these results, from measurements at angles between  $15^\circ$  and  $34^\circ$ , combined with some older data at  $6^\circ$  and  $10^\circ$ ,<sup>27)</sup> they find that  $R$  is  $\sim 0.5$  or less, everywhere in the region of measurement.<sup>28)</sup> At low values of  $\omega$ ,  $\nu R$  is approximately constant at a given value of  $\omega$ , as expected from the quark lightcone algebra, whereas at large  $\omega$ ,  $\nu R$  appears to be increasing with  $Q^2$  rather quickly, as

shown in Fig. 11. In order to reach large  $\omega$ ,  $Q^2$  is rather small, and the effects could be due to "turn on". Work is continuing on this data set, and more results are expected soon. SLAC (Group A) now has an independent set of data at angles from  $4^\circ$  to  $60^\circ$  and will generate similar information.

From the time of the first  $R$  determinations,<sup>29)</sup> it has been clear that  $\nu W_2$  is not a function of  $\omega$  in the kinematic region covered, but that systematic deviations from scaling in  $\omega$  occurred at small values of  $W$ . These deviations could be removed by assuming that scaling holds in  $\omega' = \omega + M^2/Q^2 = W^2/Q^2 + 1$  so that

$$\nu W_2(Q^2 > 1) = F_2(\omega') \text{ to } \sim 10\%$$

Since  $\lim_{Q^2 \rightarrow \infty} \omega' = \omega$ , this has no consequences for the theory. There was even a bonus in that  $F_2(\omega')$  appeared to average nicely over  $\nu W_2$  in the resonance region,<sup>17)</sup> including the elastic peak. Scaling in  $\omega$  can never "average" the elastic peak since  $F_2(\omega) = 0$  when  $W = M_P$ .

If one takes this averaging seriously, one can evaluate integrals over the data of the form

$$B_n(Q^2) = \int \frac{d\omega'}{\omega'^{2n+2}} \nu W_2^P(\omega', Q^2) \quad (9)$$

as Bloom did in 1973.<sup>30)</sup> The condition for true Bjorken scaling is that all  $B_n$  should approach a finite nonzero limit as  $Q^2$  increases without limit. Low moments (e.g.,  $B_0$  in Fig. 12a) appear quite flat for  $Q^2 > 1.5$  (GeV/c)<sup>2</sup>. Higher moments (e.g.,  $B_3$  in Fig. 12b) are not quite flat, but the contribution of the elastic peak and the resonance region is larger, and conclusions depend heavily on the "averaging" assumption implicit in the procedure. (Bloom's analysis included most of the MIT-SLAC (SFG) experiment at  $18^\circ$ ,  $26^\circ$ ,  $34^\circ$  and a preliminary version of the SLAC (Group A)  $4^\circ$  data and so is still fairly up-to-date).

There is really no evidence for scale breaking in  $\nu W_2$  in the MIT-SLAC (SFG), SLAC-MIT, or SLAC (Group A) results, when  $R$  is taken to be .16-.18 everywhere in the  $Q^2, W$  plane, and  $\omega'$  is used as the scaling variable.  $\nu R$  behaves as expected in scaling theories for small values of  $\omega$  but is not a function of  $\omega$  for large  $\omega$ , rising with increasing  $Q^2$  at constant  $\omega$ .

In an interesting paper last year,<sup>26)</sup> the MIT-SLAC (SFG) group investigated the consequences of assuming that the non-scaling in  $\omega$  was not due to terms of order  $M^2/Q^2$  in the scaling variable (and, therefore, could not be "repaired" by changing to  $\omega'$ ) but rather was due to scale breaking. They obtained coefficients for several proposed kinds of breaking, giving estimates for the parameters of different kinds of breaking. For example, in fitting to a form  $F(Q^2) = a(1 - 2Q^2/\Lambda^2)$ , suggested by the postulated parton form factors,<sup>19)</sup>  $\Lambda$  turns out to be around 8 GeV. This is another way of describing the difference between  $\nu W_2$  scaling in  $\omega$  and  $\omega'$ . One can trade changes in variable for changes in the parameters of scale breaking theories. The reader is referred to the original paper<sup>26)</sup> for the details of fits to other scale breaking hypotheses.

During the past year, SLAC (Group A) has published results from measurements at  $4^\circ$ .<sup>11)</sup> Among other things, the data give new information about the turn-on of  $\nu W_2$ . The data are shown in Fig. 13 and can be approximated by a single function in  $Q^2$ . This  $Q^2$  dependence can be factored out from  $\omega'$  dependence and can be approximated by

$$\nu W_2(Q^2, W) = \left[ 1 - W_2^{\text{el}}(Q^2) \right] F_{2P}(\omega') \quad (10)$$

where

$$W_2^{\text{el}}(Q^2) = \frac{G_E^2(Q^2) + \tau G_M^2(Q^2)}{1 + \tau}, \quad \tau = Q^2/4M^2 \quad (11)$$

Any respectable theorist will tell you that a "closure" relation like this cannot be applied to a relativistic system, so this is just a convenient way to remember how  $\nu W_2$  behaves as  $Q^2 \rightarrow 0$ .

In any case, the form is a reasonable fit to the data, so we have used the expression to estimate  $\nu W_2$  for large values of  $\omega'$ , even though the data do not reach values of  $Q^2$  where scaling "holds." The results of this are shown in Fig. 14. Extrapolation from data wholly outside the scaling region ( $Q^2 < 1$ ) begins at  $\omega' \sim 25$ , so above this value the specific form of Eq. (10) is important. Data at large values of  $\omega'$  have always tended to decrease for values of  $\omega' > 6$ . There has been suspicion that this decrease was an artifact of "turn on." The new data suggest that this is not the case, and that there is a maximum in  $\nu W_2$  at  $\omega' \sim 6$ .

The most recent single arm experiment at SLAC<sup>13)</sup> completed data taking about a year ago. Data were taken at  $50^\circ$  and  $60^\circ$  using the 1.6 GeV spectrometer, reaching values of  $Q^2$  near  $30 \text{ (GeV/c)}^2$  but limited to values of  $\omega < 2$  (Fig. 15). At large angles,  $W_1$  can be extracted from the data without detailed knowledge of R if R is small. For these kinematics

$$W_1(R=R) \approx W_1(R=0) (1 - 2E'R/E_0) \quad (12)$$

If  $R < 0.5$ , then  $W_1$  is determined within about 5% at  $60^\circ$  and 20 GeV incident. We assume  $R = .18$  and extract  $W_1$  from the measured cross sections. In a model where the scattering takes place on spin  $\frac{1}{2}$  and spin 0 (glue) constituents,  $W_1$  is determined by the properties of the spin  $\frac{1}{2}$  particles while  $W_2$  includes additional contributions from spin 0 particles. If the simple pictures of the proton have any validity, we expect  $W_1$  to scale at least as well as  $\nu W_2$ . We can compare our values of  $W_1$  with a prediction based on  $\nu W_2$  measured at smaller angles and our assumed value of R since from Eq. (5) and the definition of R

$$(W_1)_{\text{predicted}} = \nu W_2 \frac{Q^2 + \nu^2}{\nu Q^2 (1+R)} \quad (13)$$

The values of  $W_1$  and the "prediction" are shown in Fig. 16. The agreement is reasonable over nearly three decades in the value of  $W_1$ , but  $W_1$  tends to fall somewhat lower than the prediction at large values of  $Q^2$ . Of course,  $W_1$  will not scale exactly if  $\nu W_2$  scales and R is constant. The differences are small, as shown in the figure by "prediction" for different energies.

A clearer picture of  $W_1$  behavior can be obtained from Fig. 17. Here values of  $W_1$  measured for each incident energy are plotted against  $Q^2$ . The measurements are binned in  $\omega'$  and particular values of  $\omega'$  are connected by straight lines. If  $W_1$  scales, the connecting lines should be horizontal. Obviously  $W_1$  is not scaling. We can re-examine the assumption about R in the hope that some other behavior of R will restore scaling. Increasing R lowers the extracted value of  $W_1$ . By decreasing R to zero at high  $Q^2$  we can raise the values of  $W_1$  about 3% in this region and by raising R at low  $Q^2$ , values of  $W_1$  can be lowered. Unfortunately, in order to make this data scale, R would have to be approximately 2 in the low  $Q^2$  region, which conflicts with measurements of R in this region. (The correct way to show this is to include the new measurements in the evaluation of R, but that program is not yet complete.) The conclusion is that variations in R cannot change the values of  $W_1$  so that  $W_1$  is just a function  $\omega'$ .

A more quantitative measure of this non-scaling can be obtained by fitting the  $Q^2$  slope of  $W_1$  at each value of  $\omega'$  in Fig. 17. The results to a fit of the form  $a(1 + bQ^2)$  are shown in Fig. 18. Each

measured slope should be zero for scaling to hold. Figures 18a, 18b, and 18c show the effects of using different scaling variables. Fig. 18a shows that scale breaking will be even worse in  $\omega = 2M\nu/Q^2$ , the original Bjorken variable. Fig. 18c shows that  $W_1$  can be made to scale in a new ad hoc variable  $\omega_s$ , which is similar in form to  $\omega' = \omega + M^2/Q^2 = \omega + 0.88(\text{GeV}/c)^2/Q^2$ .

$$\omega_s = \omega + \frac{1.42(\text{GeV}/c)^2}{Q^2} \quad (14)$$

This is not very satisfactory, particularly since  $\nu W_2$  does not appear to scale in  $\omega_s$ . Perhaps even more unpleasant is the behavior of  $W_1$  at low values of  $\omega_s$ . In a fit of the form

$$W_1 = \sum_{n=3}^{n=6} a_n (1-x_s)^n \quad (15)$$

the coefficient  $a_3$  is small and compatible with zero, while  $a_4$  is large and positive. This is incompatible with the Drell-Yan-West<sup>31,32)</sup> relationship. The same dependence holds for  $\omega'$  fits except that the  $\chi^2$  is larger and  $a_5$  and  $a_6$  are more important.

The choice seems to lie between a somewhat artificial search for more complicated variables in which  $W_1$  and  $\nu W_2$  scale and accepting some scale breaking (perhaps due to nonleading terms). I'm sure that both alternatives will be explored. For the present, it seems less confusing to express the non-scaling in terms of the experimental numbers and  $\omega'$  scaling with  $R = .18$ , rather than as parameters for a particular theory expressed in a particular variable. Our data for  $W_1$  fall 30-40% low at  $Q^2 \sim 25-30(\text{GeV}/c)^2$  compared with our expectations based on  $\nu W_2$ .

All the recent measurements have included measurements on deuterium so that structure functions for the neutron can be extracted. Fig. 19 is a composite of available results on the ratio  $n/p$ .<sup>11,13,32)</sup> The  $50^\circ$  and  $60^\circ$  data are preliminary and assume  $R_p = R_d = .18$ . The data are crowding the current algebra limit of  $\frac{1}{4}$ , but there is no evidence that the limit is violated.

The comprehensive studies of data being undertaken independently by MIT-SLAC (SFG) and SLAC (Group A) should provide new checks of  $R_d$  and  $R_p$  and new comparisons of deuterium and neutron scaling. It is obviously of great interest to know how  $D_2$  behaves in the region where  $W_1$  exhibits non-scaling behavior.

### MUON SCATTERING

Knowledge of  $\nu W_2$  for deuterium is necessary for a clean comparison of data from SLAC and the NAL data taken with Fe targets. Before describing some of the recent results from this experiment, I want to consider three topics which are relevant to the comparison of their muon data with the electron data:  $\mu$ -e universality, 2-photon exchange processes, and A-dependence.

#### $\mu$ -e universality

The past two years have seen the publication of several results from a series of muon experiments at BNL involving experimenters from Rochester, Columbia, Harvard, and NAL. These new results add considerably to previous results<sup>33)</sup> and taken together present a picture of  $\mu$ -nucleon scattering very similar to that obtained with electrons. Radiative corrections tend to be considerably smaller for  $\mu$ -meson scattering, so the general agreement is welcome confirmation that there are no gross errors in the radiative corrections to electron experiments. Quantitative expressions of possible  $\mu$ -e differences can be obtained in both elastic and inelastic scattering experiments.

For elastic scattering<sup>34)</sup> the  $\mu$  results are shown in Fig. 20 and show a small systematic trend away from careful fits to e-p data (the "dipole" curve in the figure is actually slightly modified to represent the e-p data more closely). The data are fit to a form

$$r(Q^2) = \frac{G_{\mu p}^2(Q^2)}{G_{ep}^2(Q^2)} = N(1+Q^2/\Lambda^2)^{-2} \quad (16)$$

where N is a normalization parameter and  $\Lambda$  is a possible difference parameter. The results are presented in Fig. 21, and a value of  $1/\Lambda^2 = 0.051 \pm 0.024 (\text{GeV}/c)^{-2}$  results from the fits. The authors conclude that possible deviations are not proven, and that other experiments (g-2,  $e^+e^-$  annihilation to  $\mu^+\mu^-$ , inelastic (see below), etc.) provide little if any corroborative support for this large a deviation from universality. Some preliminary data presented at London last year by the Santa Cruz-SLAC collaboration showed good agreement between e's and  $\mu$ 's.<sup>35)</sup> Nevertheless, as for some years past, the elastic results continue to nag us for a definitive experiment.

In another paper<sup>36)</sup> results are given for  $d^2\sigma/dQ^2 d\nu$ , as shown in Fig. 22. The agreement with electron scattering is quite good, as demonstrated in Fig. 23, where the parameters of an overall fit similar to the elastic case are given for the BNL experiment and a combination of this experiment and the older experiment from SLAC.<sup>33)</sup>

#### Two-photon effect

A comparison of  $\mu^+$  and  $\mu^-$  scattering from beryllium has been made in a search for two-photon exchange amplitudes.<sup>37)</sup> The experiments measure only the real part of a two-photon amplitude. The results are shown in Fig. 24b, and there is no evidence for any asymmetry between  $\mu^+$  and  $\mu^-$ . Similar experiments have been done recently with electrons and positrons on  $H_2$  and  $D_2$ . A group from the UC-Santa Barbara campus quote a result of<sup>38)</sup>  $e^+/e^- = 1.000 \pm .003$  for scattering from hydrogen in the  $Q^2$  range from 1 to 3  $(\text{GeV}/c)^2$ , as a by-product of their search for wide-angle bremsstrahlung from deep inelastic collisions. Recently, SLAC (Group A) has results on  $e^+/e^-$  yields out to  $Q^2 = 15 (\text{GeV}/c)^2$ , as shown in Fig. 24a. I must emphasize that the figure shows the ratio of yields, not cross sections. At high values of  $Q^2$  there are contributions to the yield from other processes of up to half the total yield. To extract a limit for the ratio 2-photon to 1-photon amplitude, one must (a) assume that the backgrounds have no asymmetry, and (b) increase the error proportionately.

The Cornell-MSU-Princeton collaboration have compared the scattering of 150 GeV  $\mu^+$  and  $\mu^-$  in the Fermilab experiment and detect no asymmetry with an accuracy of better than 5%.<sup>39)</sup>

In another contribution to the conference,<sup>40)</sup> no asymmetries were observed in comparing electron and positron-proton scattering, both elastic and inelastic, at DESY.

#### A-dependence

The interaction of the photon with nuclear matter should show shadowing whenever the interaction with vector mesons is appreciable, as was clearly discussed by Gottfried at the Cornell conference.<sup>41)</sup> Several experiments have demonstrated this shadowing in total photoproduction cross sections.<sup>42)</sup> A pretty experiment from DESY<sup>43)</sup> measuring small angle photon scattering from complex nuclei shows evidence for diffraction dips in heavy nuclei and shadowing. The quantitative agreement with VMD is not impressive, but the qualitative features of the theory are verified.



The situation for virtual photons is summarized in Fig. 25, which includes data from  $6^\circ$  electron scattering,<sup>44)</sup>  $4^\circ$  electron scattering,<sup>11)</sup> and the scattering of 7.2 GeV  $\mu$  mesons.<sup>45)</sup> The electron results have quoted systematic errors of  $\pm .02$  so that there is no positive evidence for shadowing in these data. The  $\mu$  experiment shows a definite decrease at  $\langle x' \rangle = .1$ , and the authors state that their result is in fair agreement with a generalized vector dominance model by Schildknecht.<sup>46)</sup> The disagreement between electron and muon data is mild because of possible systematics.

If shadowing is important for  $x$  (or  $x'$ )  $< 0.1$ , then significant corrections will arise for this  $x$  region in the comparison of  $D_2$  and Fe cross sections (as was stressed by Hand at London).<sup>47)</sup> Comparisons of  $\mu$  data from Fermilab and SLAC electron data are currently made assuming that no shadowing occurs. The values of  $\nu W_2$  obtained from iron should be increased if shadowing is occurring. Comparisons of high and low energies from a given target are not affected if the A-dependence is a function of  $\omega$  only ( $\omega$  and  $\omega'$  are almost equal for large  $\omega$ ).

#### Recent results

Let me now turn to recent results from the Cornell-Michigan State-Princeton experiment, which was especially designed to test scaling directly. The apparatus (Fig. 26) is itself scaled so that, at two different incident energies, particles of a given  $\omega$  pass through the same location in the apparatus. At the same time the multiple scattering is held to nearly identical values at those points where the tracks are sampled. In a publication<sup>25)</sup> last year by the collaboration, statistically significant effects in the direct comparisons between 150 and 56 GeV are barely visible. The values of  $r(150 \text{ GeV}/56 \text{ GeV})$  are somewhat less than 1 except at low  $Q^2$ . The ratio of data to "Monte Carlo" predictions based on MIT-SLAC data for  $\nu W_2$  fits the simple scaling hypothesis badly in a statistical sense. The implication is that their data are high for low  $Q^2$  and high  $\omega$  (where any A-dependence effects would make the disagreement worse) and low for high  $Q^2$  and low  $\omega$ . The data have now been more fully analyzed, and results on the direct scaling have been submitted to the conference.<sup>48)</sup> The specific problem of difference in beam shape at 150 and 56 GeV was solved by selecting 56 GeV  $\mu$ 's to produce a beam distribution similar to the distribution for 150 GeV  $\mu$ 's. If the values of  $r$  obtained are fit to a constant, the result is consistent with unity,  $r(\text{direct}) = 1.02 \pm .02$  with  $\chi^2$  of 117 for 108 degrees of freedom. Nevertheless, a look at plots of the data (Figs. 27 and 28) shows some systematic trends, and it again appears that  $r$  increases with increasing  $\omega$ , and perhaps decreases with increasing  $Q^2$ . The "nicest" fit is one in which  $r$  is not a constant but depends very slightly on  $\omega$

$$r = \left( \frac{\omega}{\omega_0} \right)^n \quad (17)$$

$$n = .096 \pm 0.028, \quad \omega_0 = 6.1^{+8.9}_{-3.6}$$

There are some additional systematic errors, the largest of which is an uncertainty in relative energy calibration which results in an error of  $\pm .056$  in  $n$ . The same data can be used in conjunction with fits to the MIT and SLAC data. Similar effects are observed, and the resulting statistical precision is better. These data are to be discussed by the authors at the conference.<sup>48)</sup>

#### Conclusions on scale breaking

In conclusion, consider Table I, which summarizes the evidence concerning scale breaking. Looking at the data from both electrons and muons, it seems safe to conclude that we are not observing perfect scaling in the simplest variable,  $\omega$ . Scaling in  $\omega'$  is better, but the evidence for  $\omega'$

TABLE I

DISCUSSION

EXPERIMENT

EVIDENCE FOR SCALE BREAKING

| In $\omega$  | $\nu W_2 \neq f(\omega)$ at low $W$ .  | All Electron Data   | The evidence is very strong that the effect exists in the data. One could eliminate low $W$ and/or blame it on non leading terms.  |
|--------------|--|---|--|
| In $\omega'$ | <ol style="list-style-type: none"> <li>1. <math>\nu R \neq f(\omega')</math> at high <math>\omega'</math>.</li> <li>2. Variation of higher moment integrals with <math>Q^2</math>.</li> <li>3. <math>2M W_1 \neq f(\omega')</math> for small <math>\omega</math> and high <math>Q^2</math> (30% effect).</li> <li>4. 150 GeV/56 GeV <math>r</math> decreases with <math>\omega</math> (30% effect). <math>r</math> increases with <math>Q^2</math> (30% effect).</li> <li>5. NAL data/Monte Carlo similar to 4.</li> </ol> | <p>MIT-SFG</p> <p>All Electron Data</p> <p>SLAC <math>50^\circ</math> and <math>60^\circ</math> Data</p> <p>NAL <math>\mu</math>'s</p> <p>NAL <math>\mu</math>'s compared with electron</p> | <p>Experimental evidence is moderately good. Low values of <math>Q^2</math> for non-scaling data offer easy "escape" from conclusion that scaling is broken.</p> <p>Depends critically on local duality assumption. Also some minor extrapolation problems.</p> <p>Experimental evidence is reasonably good. Could blame it on non leading terms.</p> <p>Overall, data is consistent with <math>r = 1</math>. Systematics could be a sizeable fraction of effect. Assumption needed for R.</p> <p>Statistics better. Systematics different from 4.</p> |

?

In  $\omega''$

scale breaking is stronger now than a year ago. On the other hand, the breaking in either variable is smooth enough, and the errors are large enough, so that we can probably find a variable in which all data scale. From there, it is not hard to see that your favorite scale breaking theory and a scaling variable of greater or less complexity can be made to fit the data. I believe that it will take a lot of insight to pick out and pursue a sensible path from here on. Clearly more accurate data from electron and muon experiments will be necessary, as well as data from related processes like  $\nu$  scattering,  $e^+e^-$  annihilation, etc. We also need to move the theoretical studies back into the  $Q^2$ ,  $W^2$  plane and begin the study of scale breaking in earnest. It is important to keep in mind that the observed scale breakings are small effects, with equivalent masses about an order of magnitude greater than the proton mass (when expressed as propagators).

## OTHER TOPICS

### Hadronic final state

Many of us expected that the final hadronic states for very virtual photons would be spectacularly different from photoproduction. This was probably a result of the different theoretical approaches to the two regions. The success of VMD in photoproduction, and of the quark algebra for the deep inelastic, seem to demand a transition region in which qualitative changes occur. From the earliest experiments,<sup>49)</sup> the most striking thing about the hadronic states in deep inelastic has been the similarity to photoproduction. Very little new data has surfaced since the London conference.<sup>4)</sup> Figure 29 shows a compilation of data on mean charged multiplicity.<sup>50-54)</sup> The multiplicity appears to be somewhat lower than photoproduction, but there is no evidence of any  $Q^2$  dependence in the electroproduction data. There appear to be several processes in which changes occur over a small range in  $Q^2 \sim 0.2(\text{GeV}/c)^2$ , including multiplicity, A-dependence,  $p\pi^0$  exclusive final state, etc. It will be interesting to see if these are somehow connected with a transition region. If so, the transition region is small, and the changes are subtle. I suspect that we will eventually find that very similar mechanisms are producing the final states in the large  $Q^2$  region and at  $Q^2 = 0$ .

The one process which shows strong and steady  $Q^2$  dependence is forward pion production.<sup>50,55-57)</sup> Figure 30 shows the present data, excluding data from UCSC-SLAC (Streamer Chamber Group), who are bringing new results to the Conference. Measurements on deuterium should provide a nice test of the quark-parton predictions.

### Total photoproduction cross section

While not strictly a part of deep inelastic scattering, the Chicago-Harvard-Illinois-Oxford collaboration have obtained a result (Fig. 31) for the total photo cross section at 100 GeV by extrapolating  $\mu$  scattering data at low  $Q^2$ . The result agrees with extrapolations from lower energy data.

### Parity nonconservation in scattering experiments

The existence of weak neutral currents is well established in neutrino interactions. Measurements of  $\nu + N \rightarrow \nu + X$  and  $\bar{\nu} + N \rightarrow \bar{\nu} + X$  are in fair agreement with gauge theories of weak interactions and the parton model. The same model predicts neutral current effects in deep inelastic lepton scattering.<sup>58)</sup> The observed asymmetries should be in the range of  $(10^{-4} - 10^{-5})Q^2$ , depending on various kinematic factors and the Weinberg angle.

In a contribution to this conference<sup>59)</sup> results are reported for an experiment in which polarized beams of 20 GeV  $\mu$  mesons from  $\pi$  decay are employed. No asymmetry was observed at levels of

$\text{few} \times 10^{-4}$ . This measurement excludes other neutral axial-vector currents (on which previous limits were quite poor) but the result is not in conflict with our present ideas about the weak neutral currents.

### CONCLUSIONS

The puzzle of deep inelastic scattering vs. annihilation has been replaced with the challenge of the new particles. Paradoxically, the evidence for the simplest quark-algebra models of deep inelastic processes is weaker than a year ago. Definite evidence of scale breaking has been found, but the specific form of the scale breaking is difficult to extract from the data, a situation which is unlikely to improve rapidly. The size of the scale breaking observed implies reasonable parameters in theories of anomalous dimensions, or in asymptotically free theories, so the general framework in which the experiments are analyzed doesn't appear to be in trouble. We have not made much progress in unraveling the mysteries of final state hadrons, although a great deal of experimental work continues. For the future, progress will depend on precise experiments at high energies together with theoretical investigations of the deep inelastic region where  $Q^2$ ,  $\nu$ , and the investment in experiments do not approach infinity.

### ACKNOWLEDGEMENTS

I wish to express my thanks to my colleagues at SLAC for their generous help in the preparation of this talk. My particular thanks go to Drs. Atwood, Prescott, and Rochester, and to Professor H. DeStaebler, without whose constructive criticism and help this manuscript would not exist. My thanks also to the Publications and Technical Illustrations Groups at SLAC for their patience and understanding help in the preparation of the manuscript. I also gratefully acknowledge the help of Ms. M. L. Arnold for her assistance and enthusiasm.

Finally, I owe thanks to the U. S. Energy Research and Development Administration and the National Science Foundation for their support.

\* \* \*

### REFERENCES

The following abbreviations will be used:

Cornell 1971

Proceedings of the 1971 International Symposium on Electron and Photon Interactions at High Energies, N. B. Mistry, editor, Laboratory for Nuclear Studies, Cornell (1972).

Bonn 1973

Proceedings of the 6th International Symposium on Electron and Photon Interactions at High Energies, H. Rollnik and W. Pfeil, editors, North Holland Publishing Co. (1974).

London 1974

Proceedings of the XVII International Conference on High Energy Physics, J. R. Smith, editor, Rutherford Laboratory (1974).

- 1) A. Litke et al., Phys. Rev. Letters 30, 1189 (1973); G. Tarnopolsky et al., Phys. Rev. Letters 32, 432 (1974).

- 2) B. Richter, Conf. on Lepton Induced Reactions, Irvine (Dec., 1973).
- 3) B. Richter, London 1974, p. IV-37.
- 4) F. J. Gilman, London 1974, p. IV-149.
- 5) J. -E. Augustin et al., Phys. Rev. Letters 33, 1406 (1974).
- 6) J. J. Aubert et al., Phys. Rev. Letters 33, 1404 (1974).
- 7) G. Feldman, this conference.
- 8) J. D. Bjorken, Bonn 1973, p.25.
- 9) Luke Mo, private communication (May, 1975).
- 10) C. Chang et al., Abstract E2-03, this conference.
- 11) S. Stein et al., Stanford Linear Accelerator Center Report, SLAC-PUB-1528 (Jan., 1975).  
Submitted to Physical Review.
- 12) J. D. Bjorken, Phys. Rev. 179, 1547 (1969).
- 13) W. B. Atwood, Stanford Thesis (June, 1975). Unpublished.
- 14) S. J. Brodsky and G. R. Farrar, Phys. Rev. D11, 975 (1975).
- 15) G. B. West, Physics Reports 18, 263 (1975).
- 16) R. G. Arnold et al., paper submitted to the 6th International Conference on High Energy Physics and Nuclear Structure, Santa Fe, New Mexico (July, 1975).
- 17) E. D. Bloom and F. J. Gilman, Phys. Rev. D4, 2901 (1971).
- 18) See for example H. J. Lipkin, Proceedings of Summer Institute on Particle Physics, Stanford Linear Accelerator Center Report SLAC-167, Vol. 1, p. 239 (Nov., 1973).
- 19) M. Chanowitz and S. D. Drell, Phys. Rev. Letters 30, 807 (1973); Phys. Rev. D9, 2078 (1974).
- 20) G. B. West and P. Zerwas, Phys. Rev. D10, 2130 (1974).
- 21) K. G. Wilson, Phys. Rev. 179, 1499 (1969).
- 22) D. J. Gross and F. Wilczek, Phys. Rev. D9, 980 (1974).
- 23) There are presently two muon scattering experiments at Fermilab:
  - a) Expt. 26.  $\mu^+$  Fe inclusive. Cornell-Michigan State-Princeton-San Diego collaboration.
  - b) Expt. 98.  $\mu^+$  p,d inclusive and exclusive. Chicago-Harvard-Illinois-Oxford collaboration.
- 24) SLAC Expt. E-80. Yale-SLAC (SFG) Collaboration.
- 25) D. J. Fox et al., Phys. Rev. Letters 33, 1504 (1974).
- 26) E. M. Riordan et al., Phys. Letters 52B, 249 (1974).
- 27) J. S. Poucher et al., Phys. Rev. Letters 32, 118 (1974).
- 28) E. M. Riordan et al., Phys. Rev. Letters 33, 561 (1974).
- 29) G. Miller et al., Phys. Rev. D5, 528 (1972).
- 30) E. D. Bloom, Bonn 1973, p. 227.

- 31) S. D. Drell and T. M. Yan, Phys. Rev. Letters 24, 181 (1970); G. B. West, Phys. Rev. Letters 24, 1206 (1970).
- 32) A. Bodek et al., Phys. Rev. Letters 30, 1087 (1973).
- 33) T. J. Braunstein et al., Phys. Rev. D6, 106 (1972).
- 34) I. Kostoulas et al., Phys. Rev. Letters 32, 489 (1974).
- 35) C. A. Heusch, London 1974, p IV-65.
- 36) A. Entenberg et al., Phys. Rev. Letters 32, 486 (1974).
- 37) H. Jostlein et al., Phys. Letters 52B, 485 (1974).
- 38) D. L. Fancher et al., Abstract E 2-04, this conference. Also D. O. Caldwell, London 1974, p IV-79.
- 39) C. Chang et al., Abstract E 2-02, this conference.
- 40) S. Hartwig et al., Abstract E 2-07, this conference.
- 41) K. Gottfried, Cornell 1971, p. 221.
- 42) a) D. O. Caldwell et al., Phys. Rev. D7, 1362 (1973).  
b) V. Heynen et al., Phys. Letters 34B, 651 (1971).  
c) G. R. Brookes et al., Phys. Rev. D8, 2826 (1973).
- 43) L. Criegee et al., Submitted to this conference.
- 44) W. R. Ditzler et al., Stanford Linear Accelerator Center Report SLAC-PUB-1543 (Feb., 1975). To be published in Physics Letters.
- 45) M. May et al., University of Rochester Report UR-532 (May, 1975).
- 46) D. Schildknecht, Nuc. Phys. B66, 398 (1973).
- 47) L. N. Hand, London 1974, p. IV-61.
- 48) L. N. Hand et al., Abstract E2-01, this conference.
- 49) K. Berkelman, Cornell 1971, p. 263.
- 50) K. Moffeit et al., Phys. Rev. D5, 1603 (1972).
- 51) J. Ballam et al., Phys. Letters 56B, 193 (1975).
- 52) V. Eckardt et al., Phys. Letters 43B, 240 (1973); Deutsches Elektronen-Synchrotron Report DESY 74/5 (Feb., 1974).
- 53) C. del Papa et al., University of California, Santa Cruz, Report 75-039 (1975).
- 54) P. H. Garbincius et al., Phys. Rev. Letters 32, 328 (1974); B. Gibbard et al., Laboratory of Nuclear Studies, Cornell, Report CLNS-266 (1974).
- 55) J. T. Dakin et al., Phys. Rev. D8, 687 (1973).
- 56) I. Dammann et al., Nuc. Phys. B54, 381 (1973).
- 57) J. Ballam et al., Stanford Linear Accelerator Center Report SLAC-PUB-1163 (Dec., 1973). Unpublished.
- 58) S. M. Berman and J. R. Primak, Phys. Rev. D9, 2171 (1974).
- 59) Y. B. Bushnin et al., Abstract E2-09, this conference.

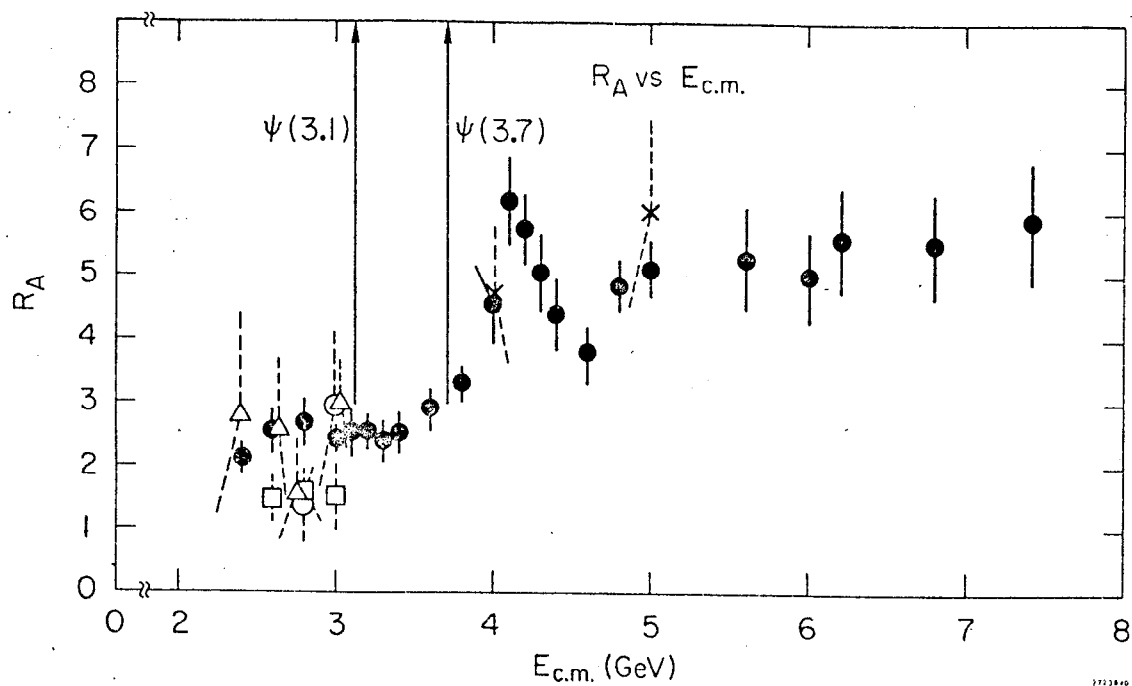


Fig. 1 The ratio,  $R_A$ , of the total annihilation cross section of  $e^+e^-$  into  $A$  hadrons to that into  $\mu$  pairs, versus center-of-mass energy,  $E_{cm}$ . (Reported to this conference by G. Feldman.)

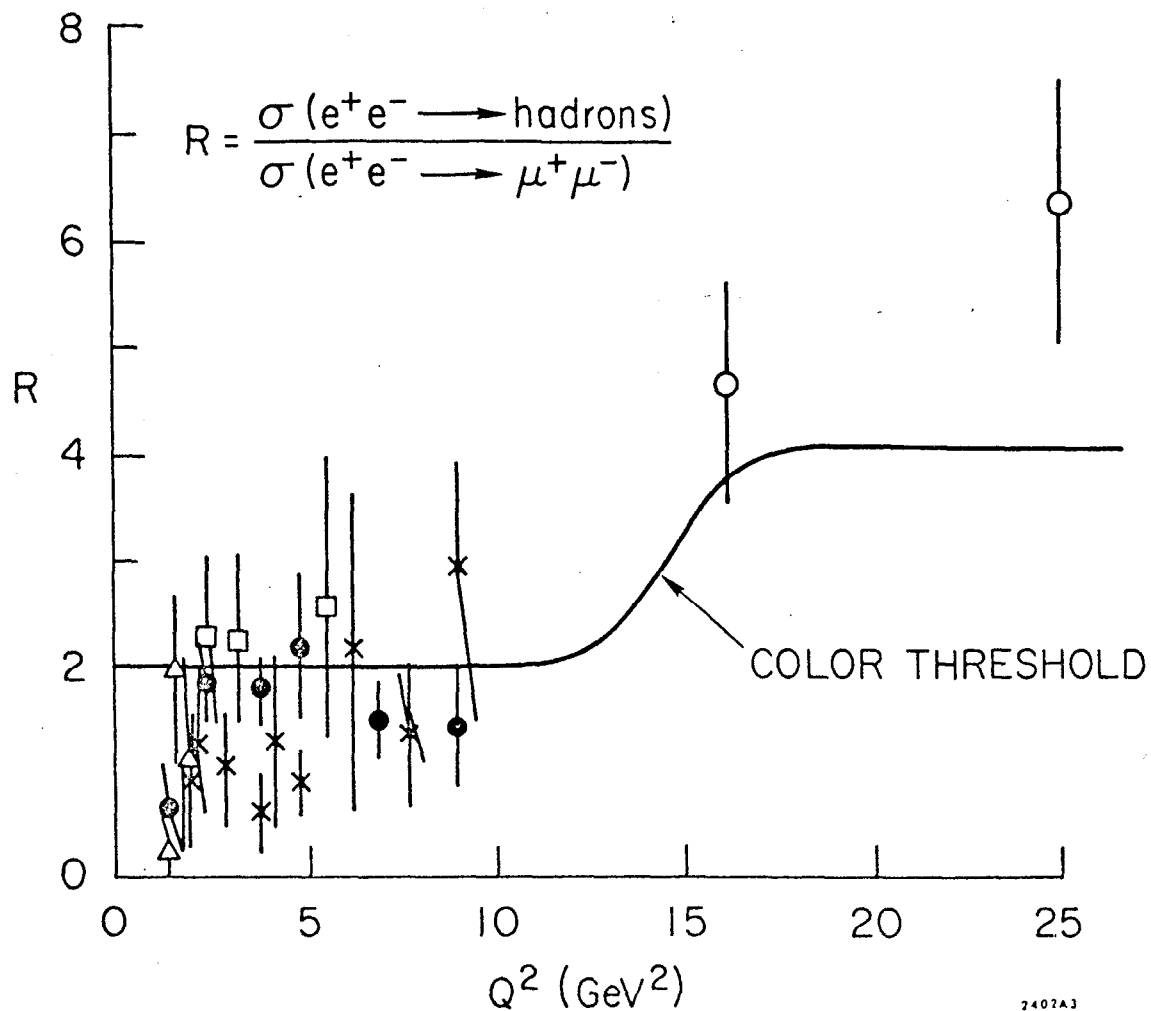


Fig. 2  $R_A$ , circa 1973, as interpreted by Bjorken at the Bonn conference.



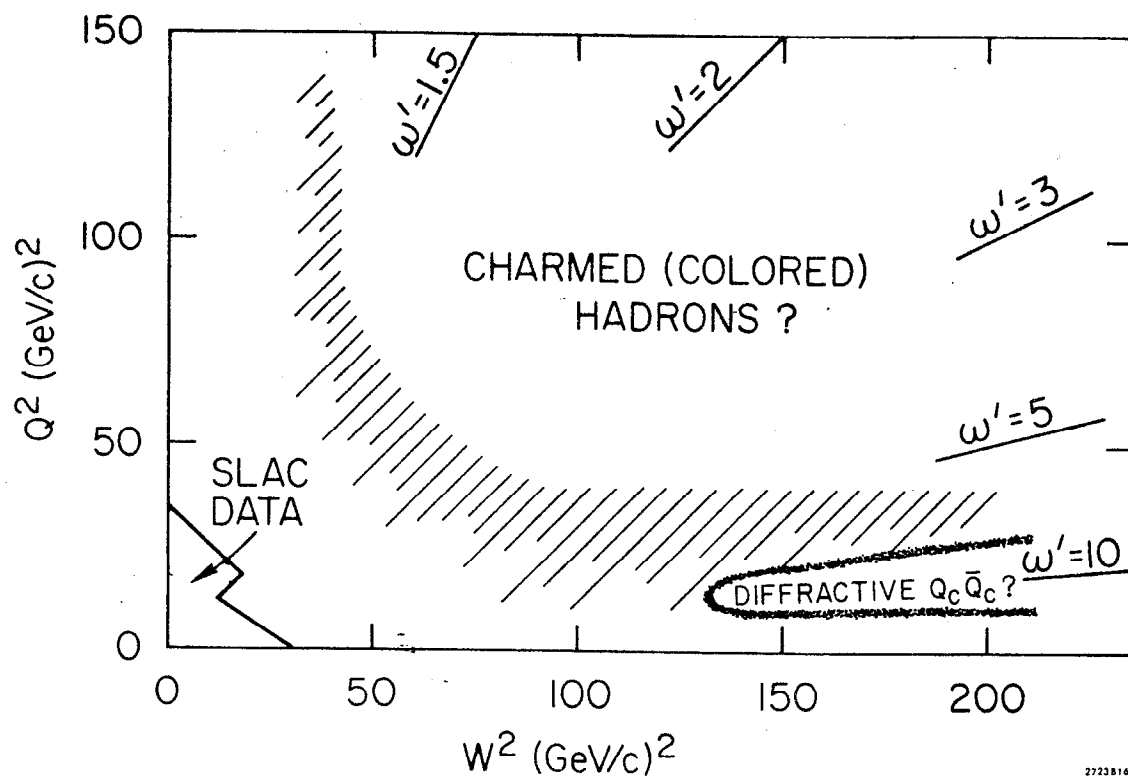


Fig. 3 Possible color and/or charm thresholds in the  $Q^2$ - $W^2$  plane.

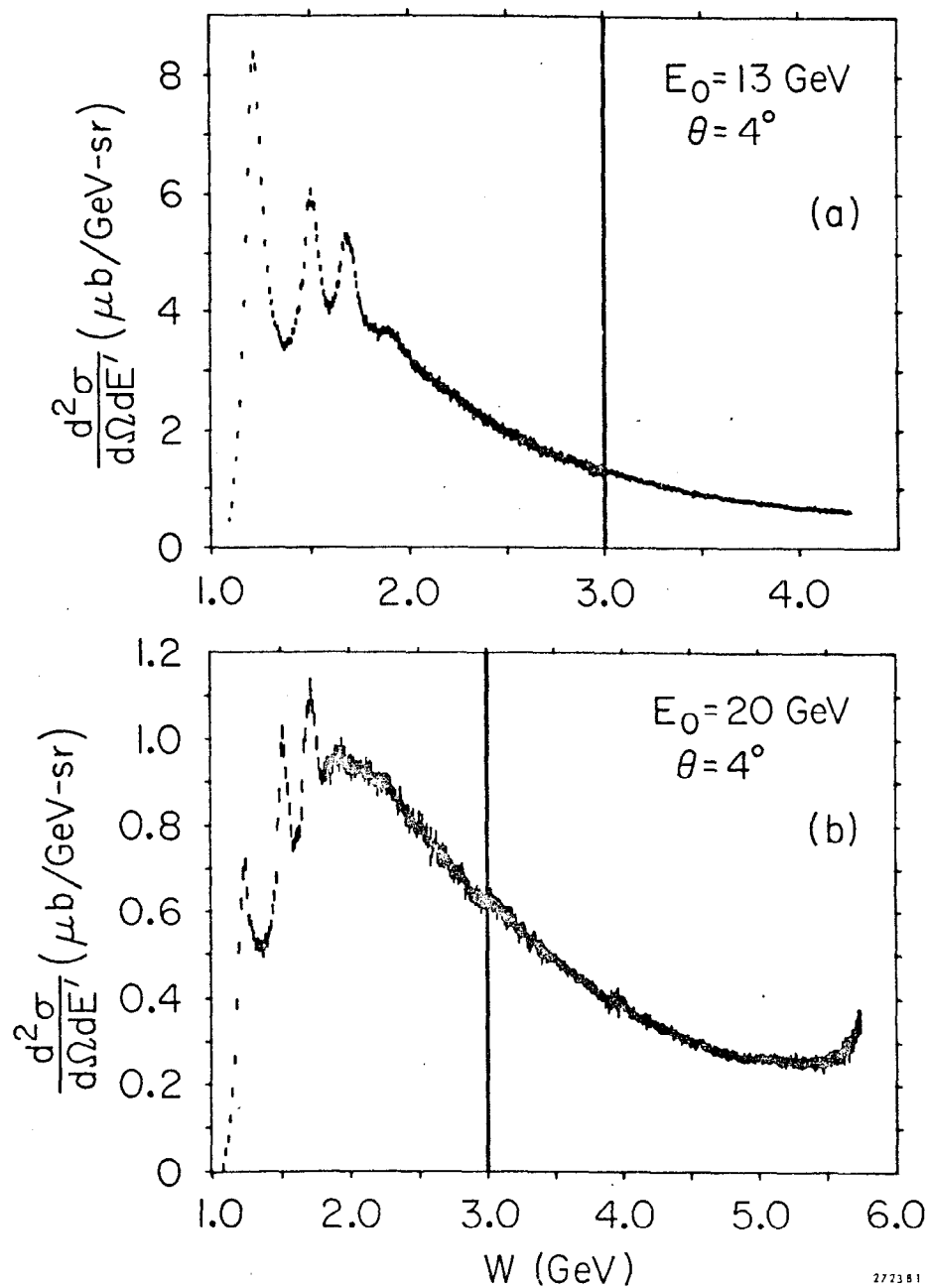


Fig. 4 Inelastic cross sections versus missing mass for incident electrons of 13 and 20 GeV scattered at  $4^\circ$ . A slight normalization discrepancy exists across the vertical bar which separates previous data from the extended data. The disturbance at  $W = 3.9 \text{ GeV}$  in the second spectrum occurs where two scans were joined and is thought to be an instrumental effect.



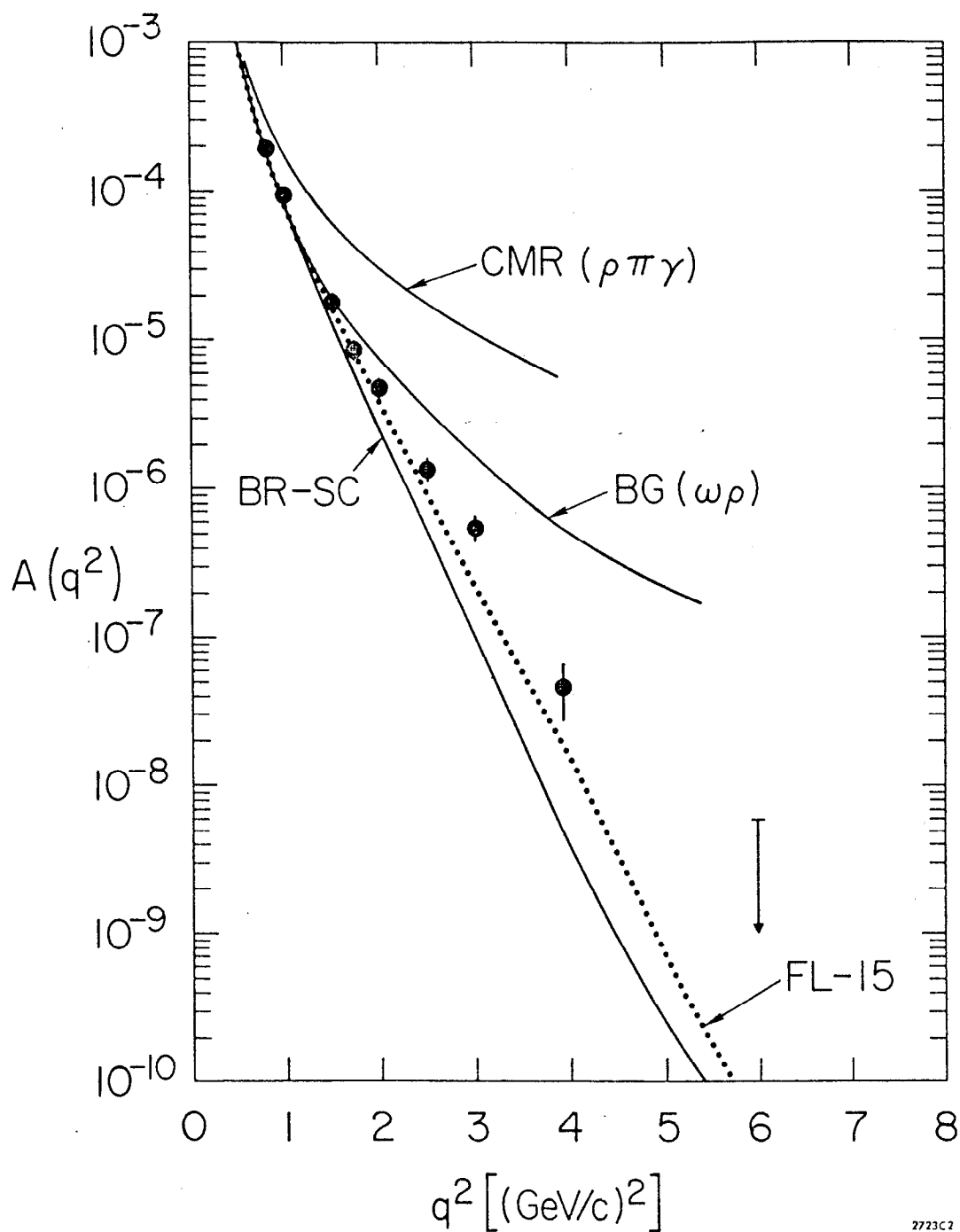


Fig. 6 The deuteron form factor  $A(q^2)$  versus  $q^2$  compared to various models. The models shown are of Chemtob, Moniz and Rho (CMR); Blankenbecler and Gunion, who were calculating an upper limit on  $A(q^2)$  (BG); Bethe-Reid soft core (BR-SC); and Feshbach and Lomon with 7.5% D state. (FL-15).

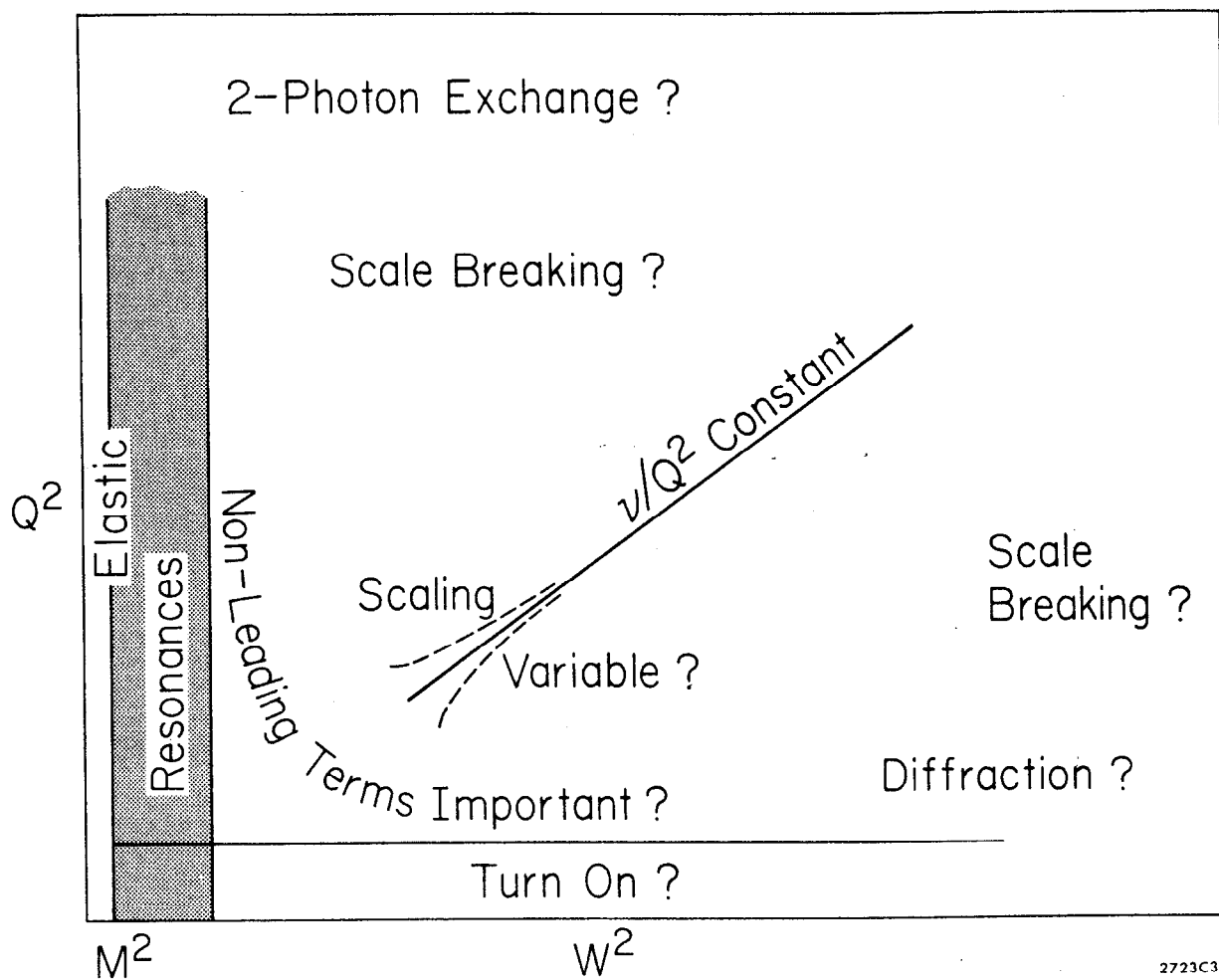


Fig. 7 The  $Q^2$ - $W^2$  plane showing regions where the data might not scale.

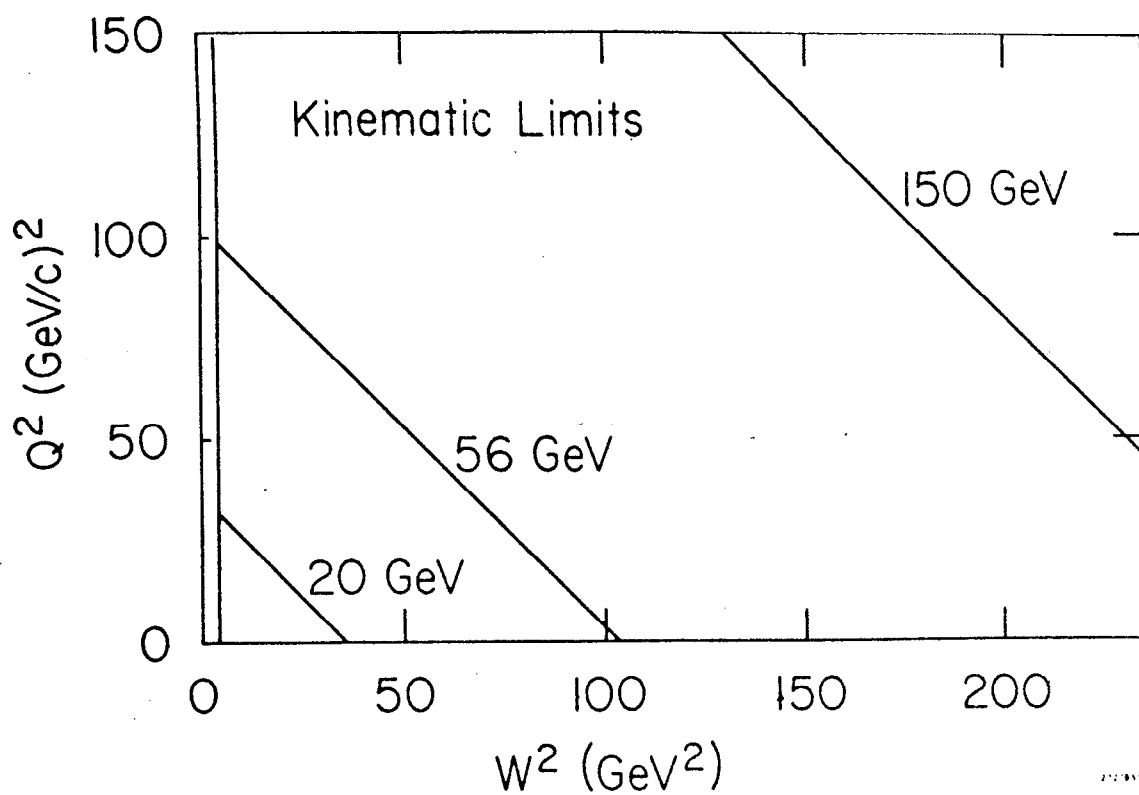


Fig. 8 Kinematic limits for inelastic scattering at incident energies of 20, 56 and 150 GeV. Practical considerations further limit the kinematic range.

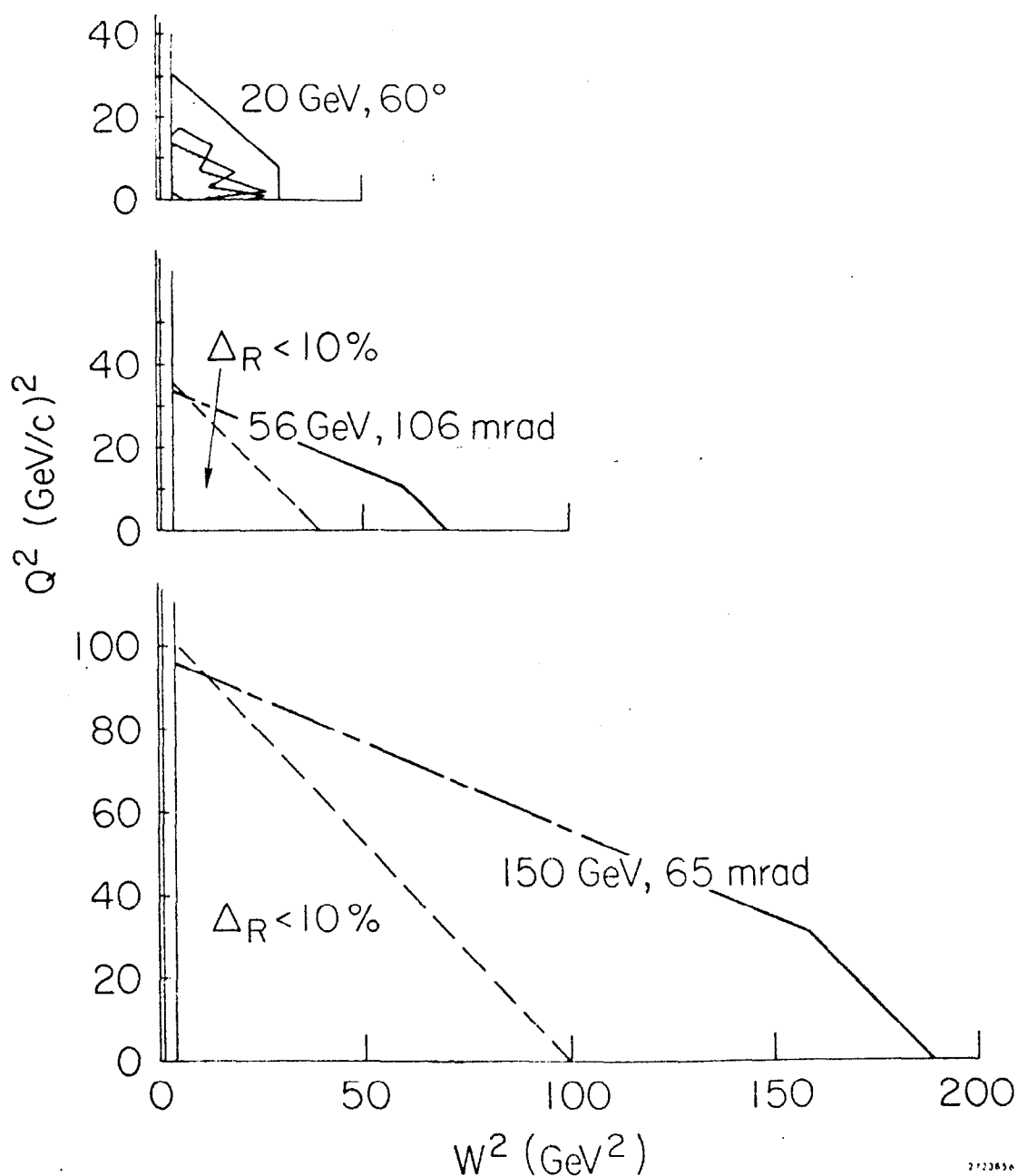


Fig. 9 Currently explored kinematic ranges for incident energies of 20, 56 and 150 GeV. The angles shown are the maximum measured at the three energies. In the regions to the left of the dashed line, changing  $R$  from 0 to  $\infty$  changes  $\nu W_2$  by less than 10%. At 20 GeV,  $R$  is already known in the corresponding region. The small cross section at high  $Q^2$  severely limits the amount of data in the dot-dashed region.

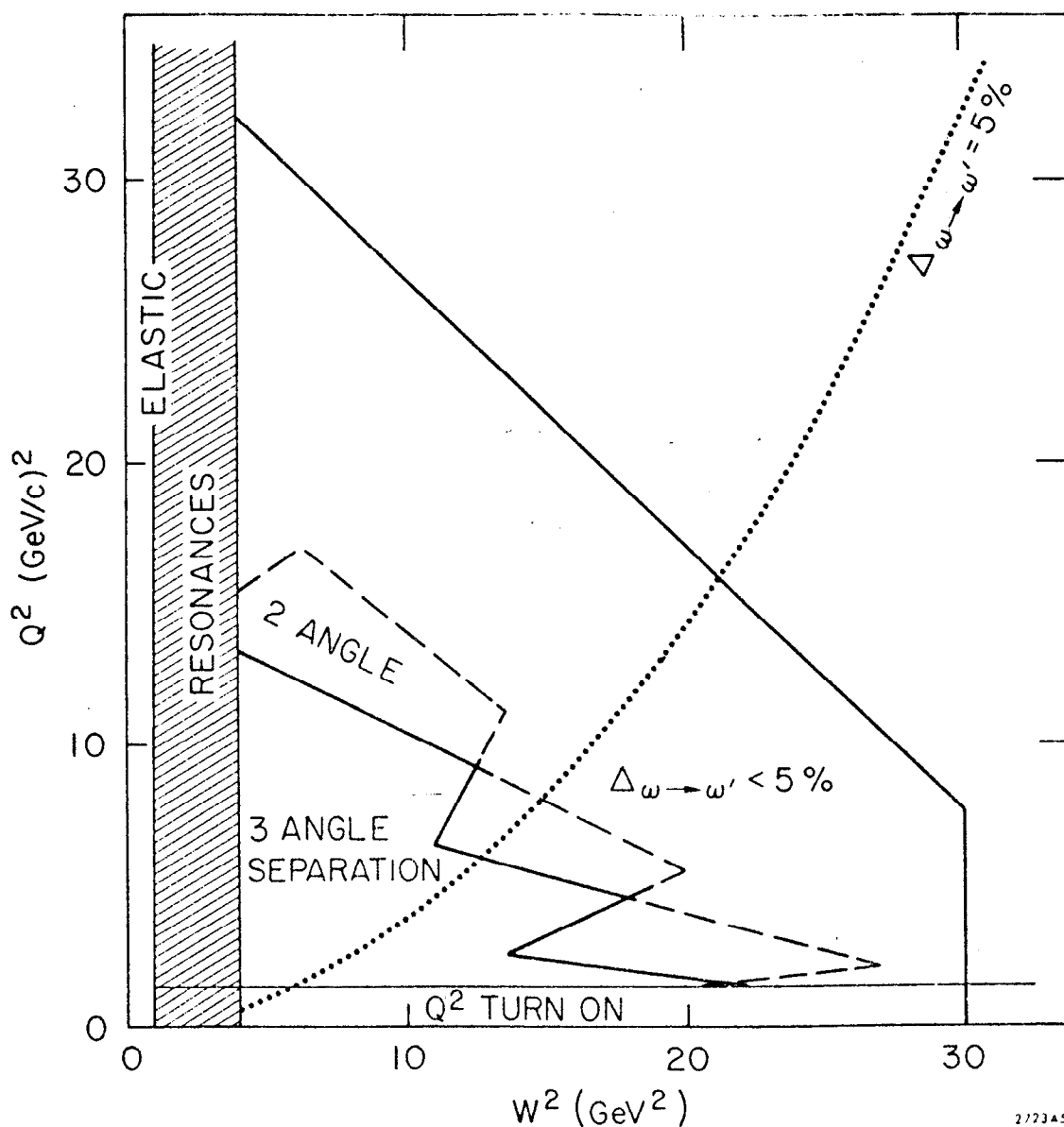


Fig. 10 Detail of Figure 9, showing the region in which R separations have been made. At least two angles are required to make a separation but, in the region indicated, three or more angles have been used. In the region to the right of the dotted line, changing from  $\omega$  to  $\omega'$  changes the calculated value of  $\nu W_2$  by less than 5%.



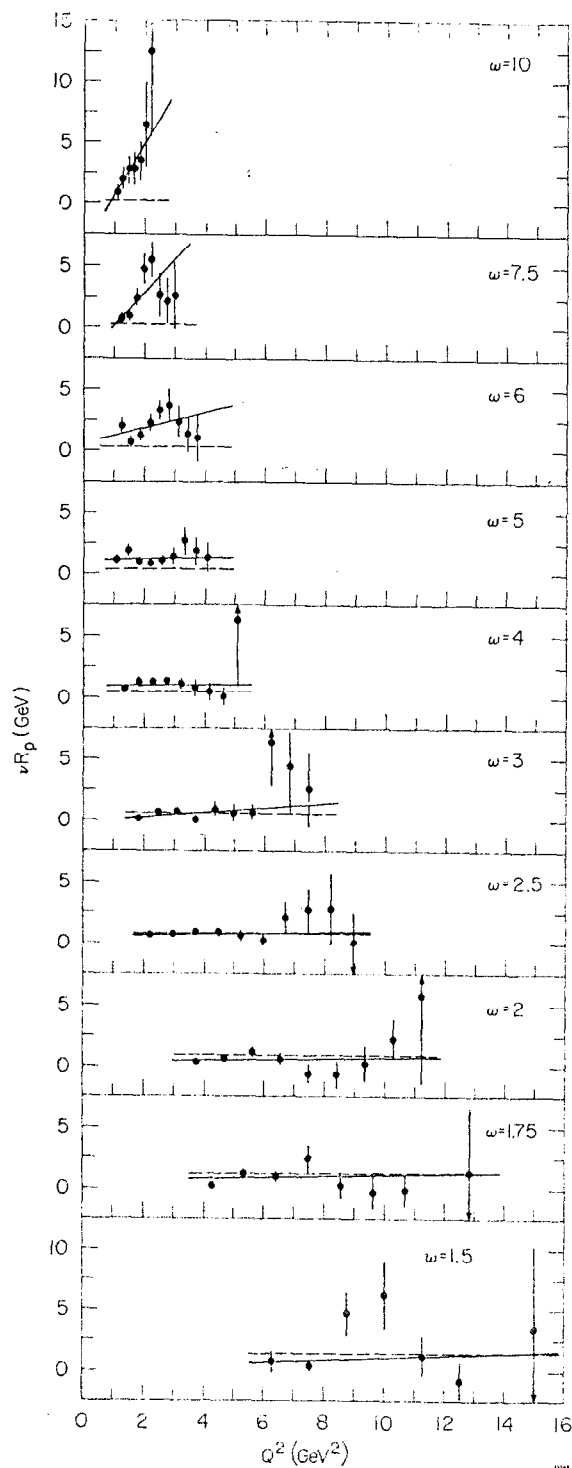


Fig. 11  $\nu R_p$  versus  $Q^2$  for values of  $\omega$  from 1.5 to 10. The solid lines are fits to  $\nu R_p = a + bv$ , and the dashed lines are  $R_p = Q^2/\nu^2$ .

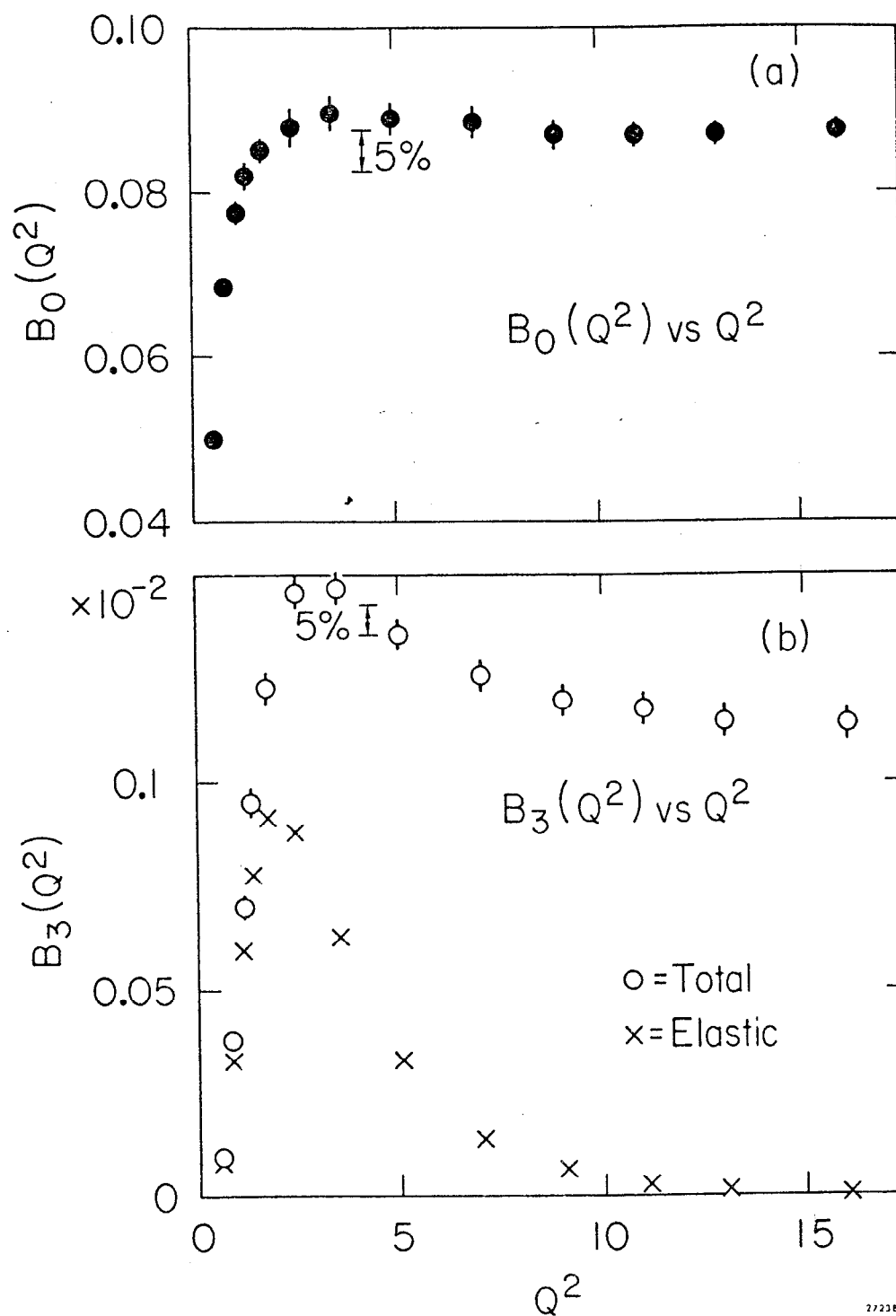


Fig. 12  $B_0(Q^2)$  and  $B_3(Q^2)$  for  $R = 0.168$ . A scaling fit in  $\omega'$  is used where no data exists. The crosses give the contribution from elastic scattering. The errors shown include estimates of systematic uncertainties.

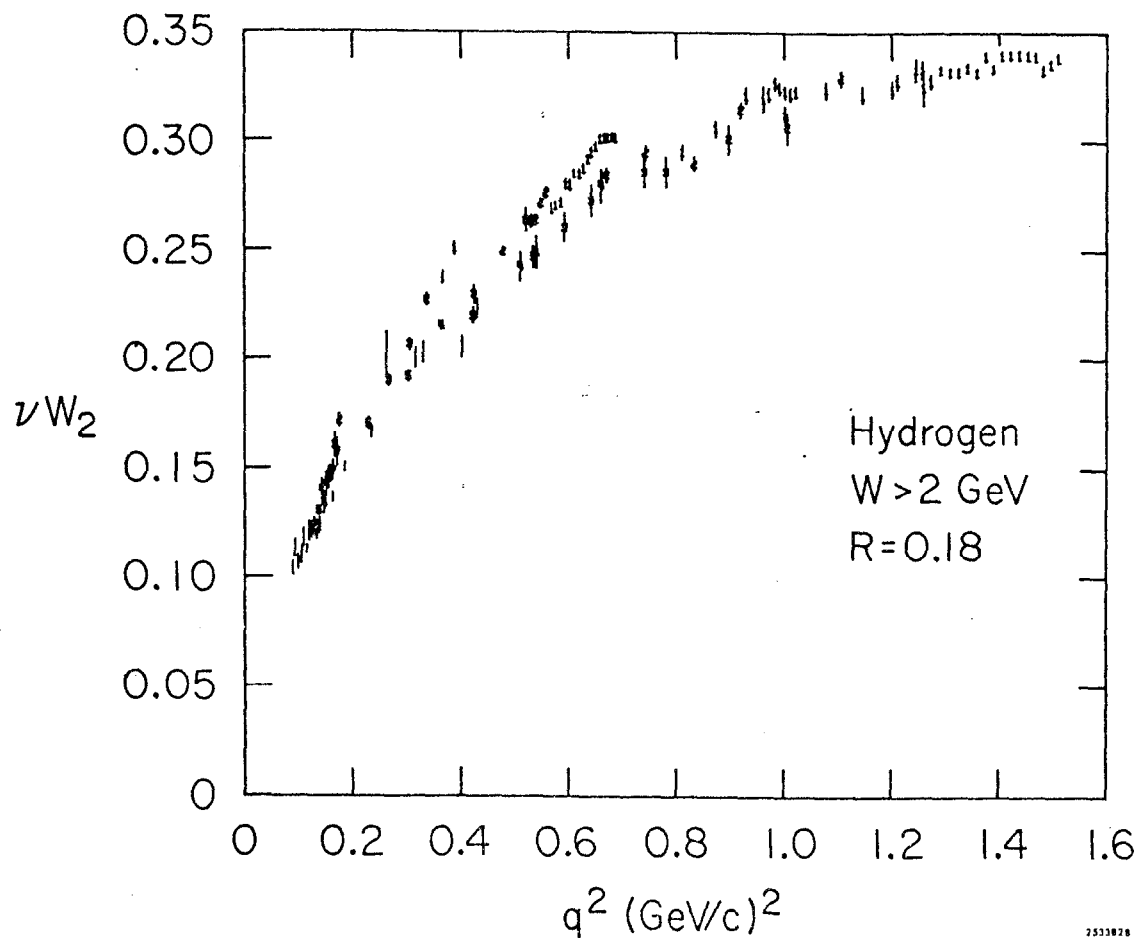


Fig. 13  $\nu W_2$  versus  $Q^2$  for  $\omega' > 6$  from data taken at  $4^\circ$ . It can be seen that the turn-on to scaling can be approximated by a single function of  $Q^2$ . The errors are statistical only. At a  $Q^2$  of 0.6,  $\omega'$  varies between about 6 and 45.

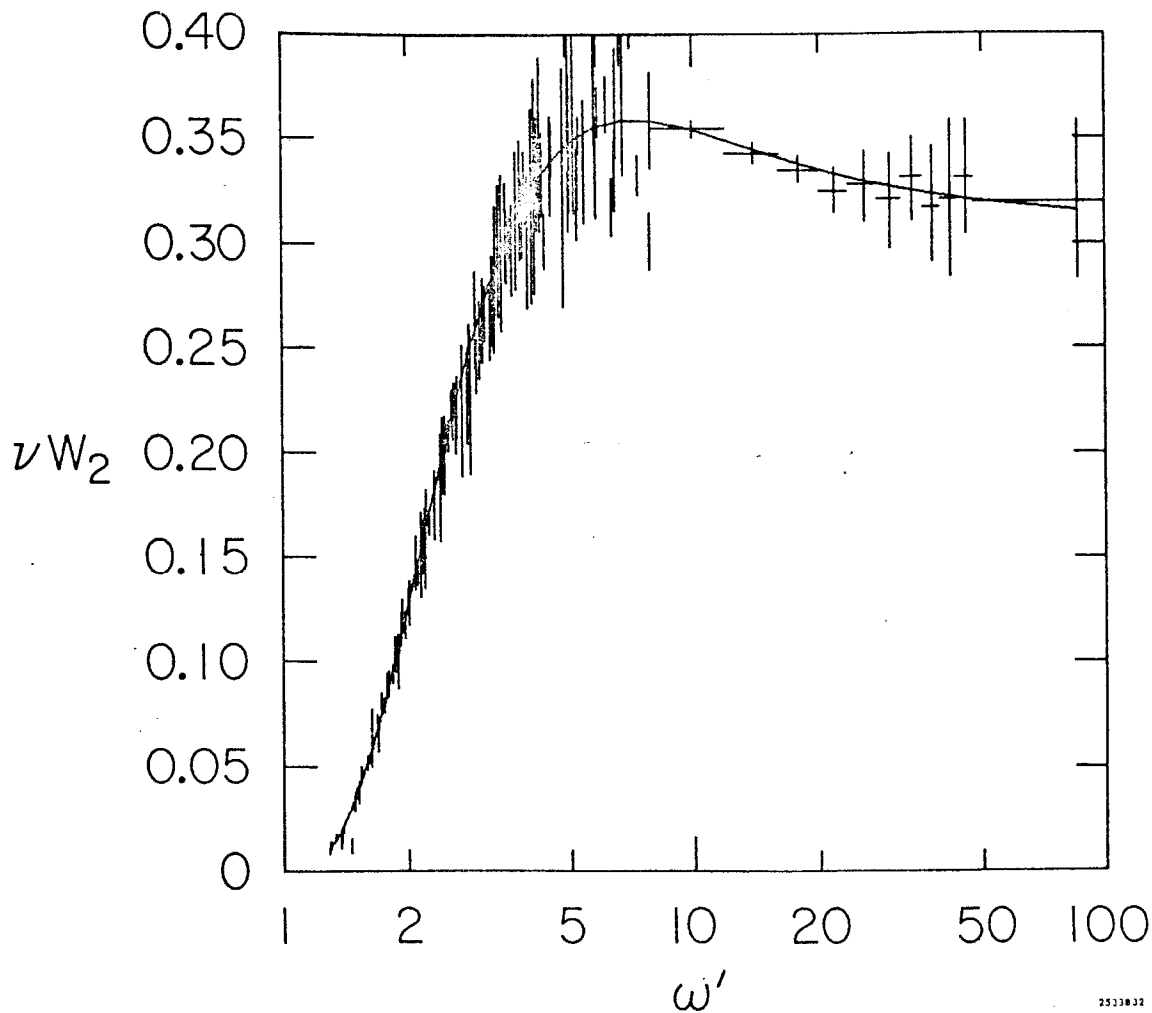
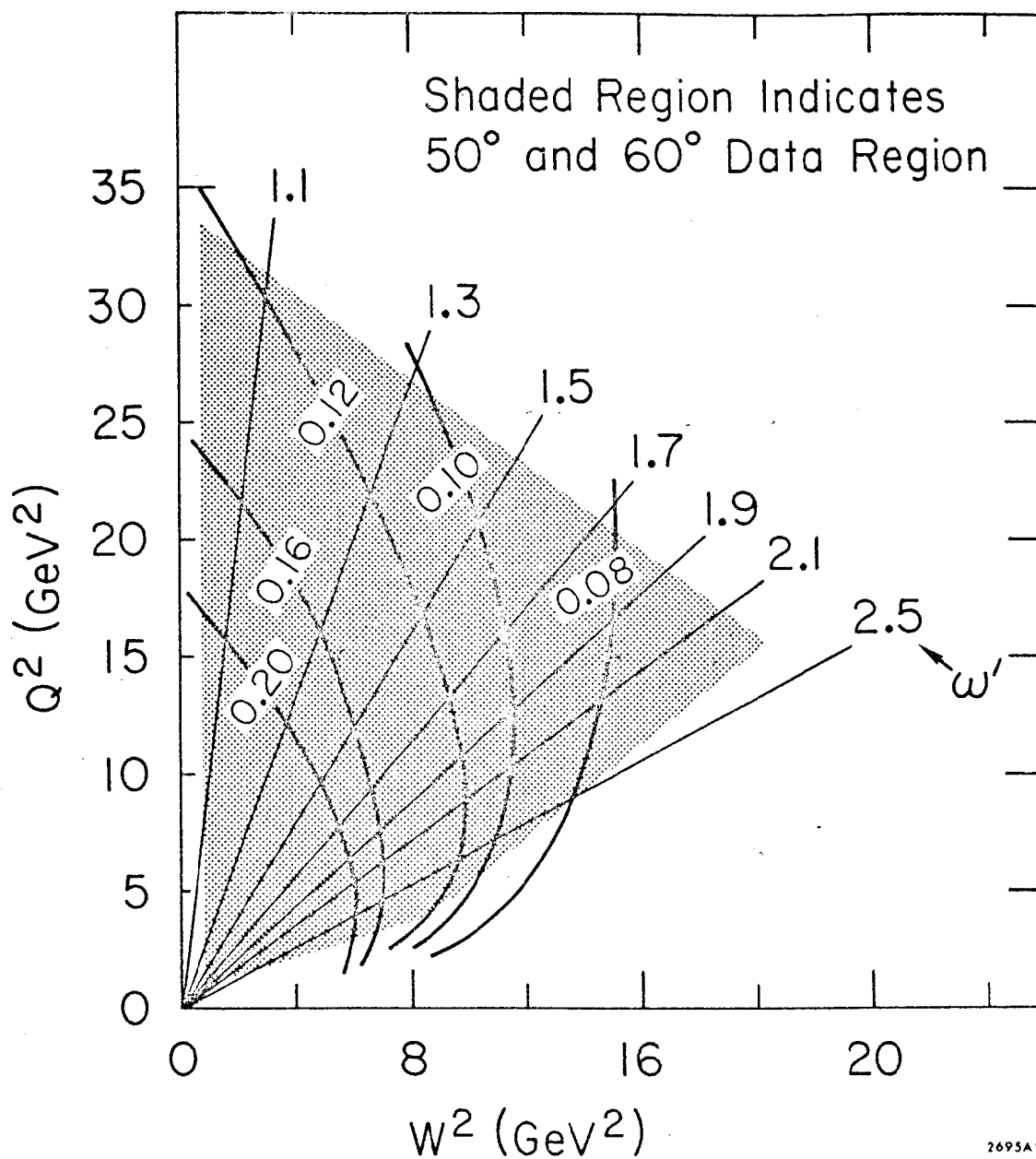


Fig. 14  $\nu W_2$  vs.  $\omega'$ .  $R$  is assumed to be 0.18 (at  $\omega'^2 = 30$ , changing  $R$  from 0.18 to 0.36 increases  $\nu W_2$  by only 5%). The data above  $\omega' = 8^2$  are extrapolated from a fit to the  $Q^2$  turn-on at each value of  $\omega'$ . The solid line is a polynomial fit to the data. Above  $\omega' = 25$ , the value of  $\nu W_2$  depends sensitively on the parameterization of the turn-on. The systematic error may be as large as 20% in the highest  $\omega'$  bin, as indicated.



2695A9

Fig. 15 The  $Q^2$ - $W^2$  plane showing the region measured in the  $50^\circ$  and  $60^\circ$  experiment. Lines of constant  $\omega'$  radiate from the origin. Also shown are curves of constant polarization parameter,  $\epsilon$ , with the levels corresponding to  $\theta = 60^\circ$ .

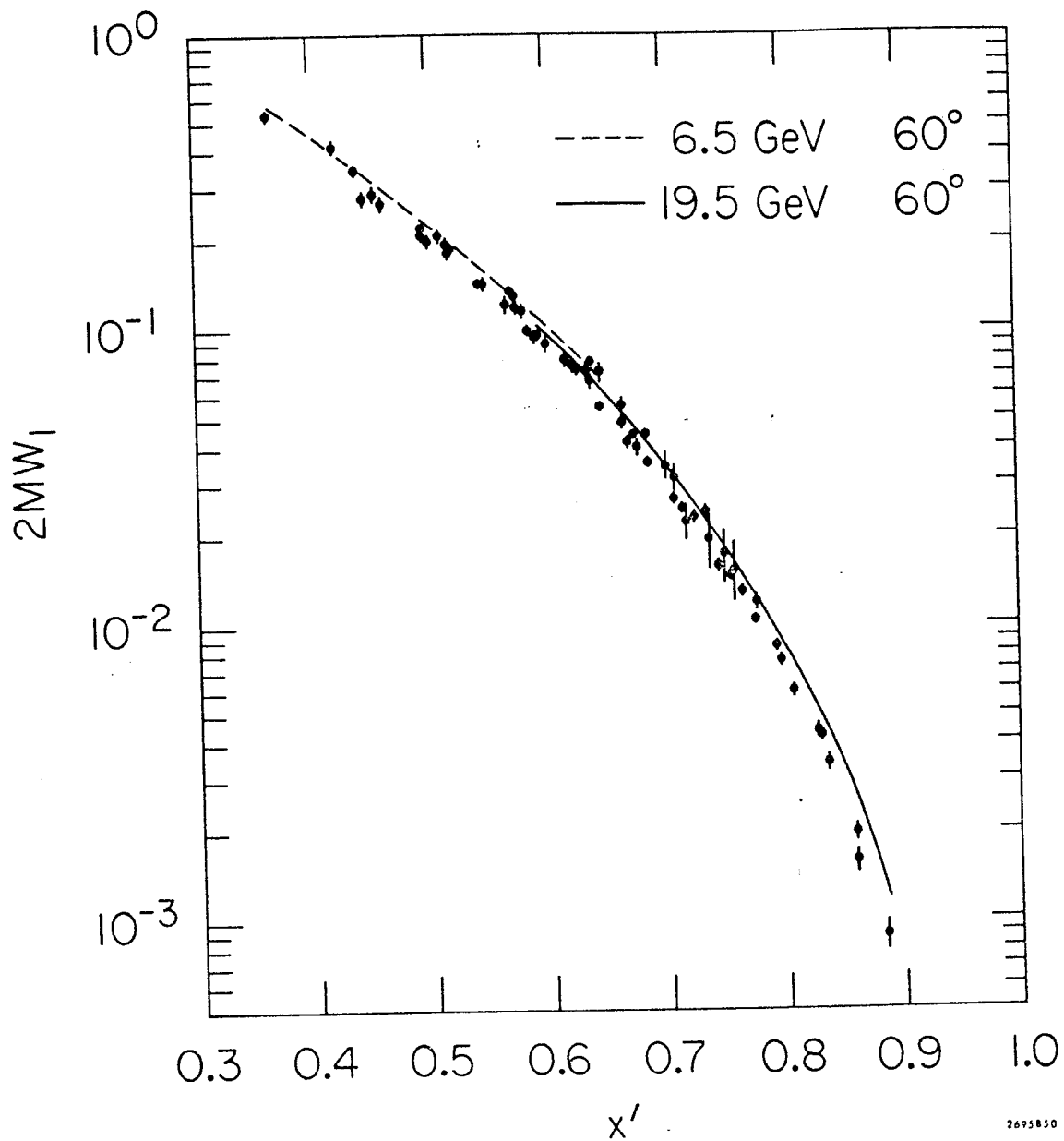


Fig. 16  $2MW_1$  vs.  $x'$  from measurements at  $50^\circ$  and  $60^\circ$ . The dashed and solid lines are "predictions" based on a scaling fit to  $\nu W_2$  and  $R = 0.18$ .

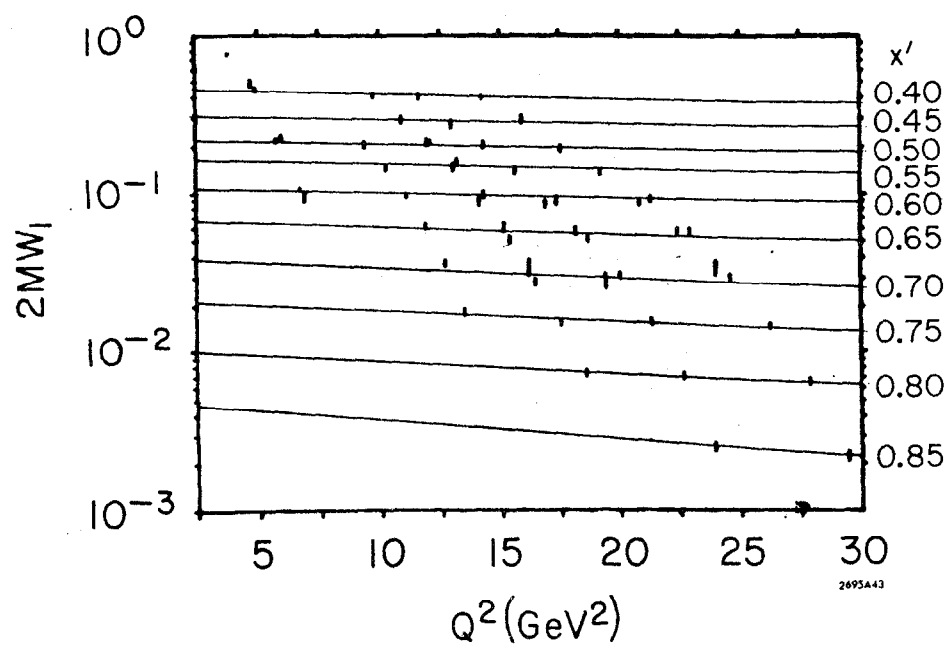


Fig. 17  $2MW_1$  vs.  $Q^2$  binned in  $x'$ . Data at the same  $x'$  are fit to a straight line in  $Q^2$ .  $W_1$  clearly does not scale in  $x'$  since all data points at a given  $x'$  should be constant in  $Q^2$ , and the connecting lines should be horizontal.

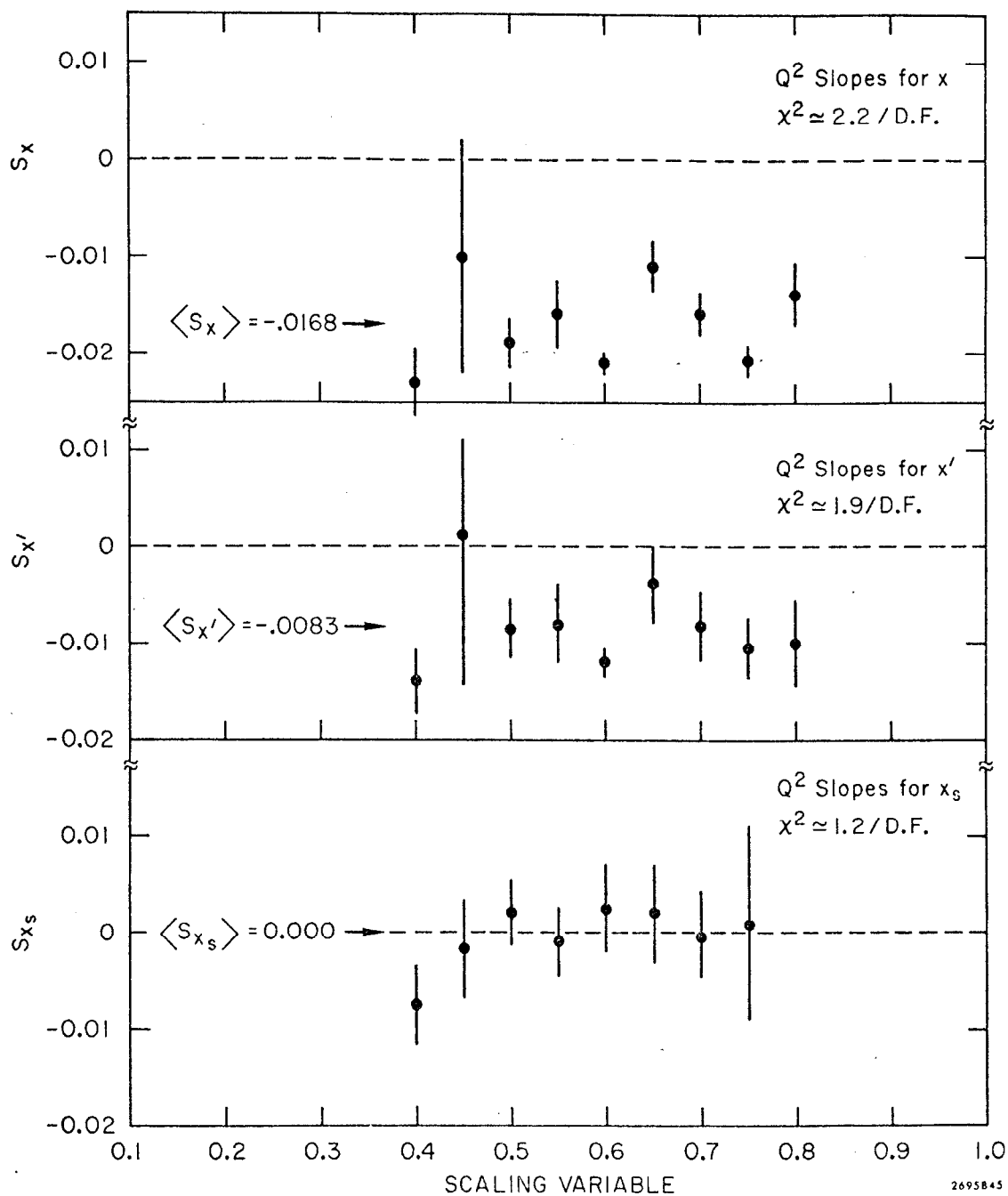


Fig. 18 Plots similar to Figure 17 were made for the variables  $x$  and  $x'$ . ( $\omega_s = 1/x_s = 2Mv + M_s^2/Q^2$ ). Plotted here are the slopes of the lines of the form  $2M\omega_s = a(1+S Q^2)$  in the variables  $x$ ,  $x'$  and  $x_s$ .  $M_s^2$  was chosen to make the average slope zero.



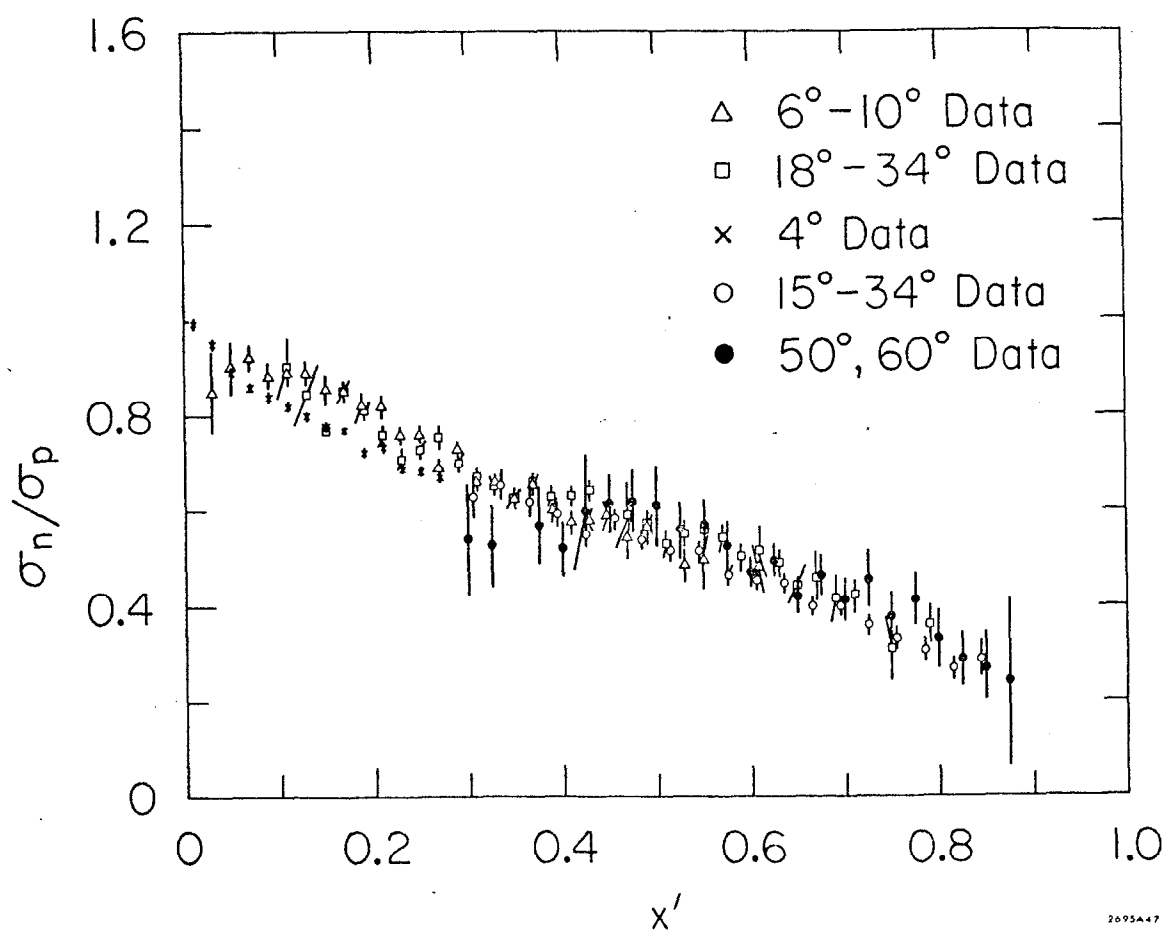


Fig. 19 The ratio of the neutron cross section (as extracted from  $D_2$  data) to the proton cross section. The effects of Fermi motion in deuterium increase the systematic errors (not included) as  $x' \rightarrow 1$ .

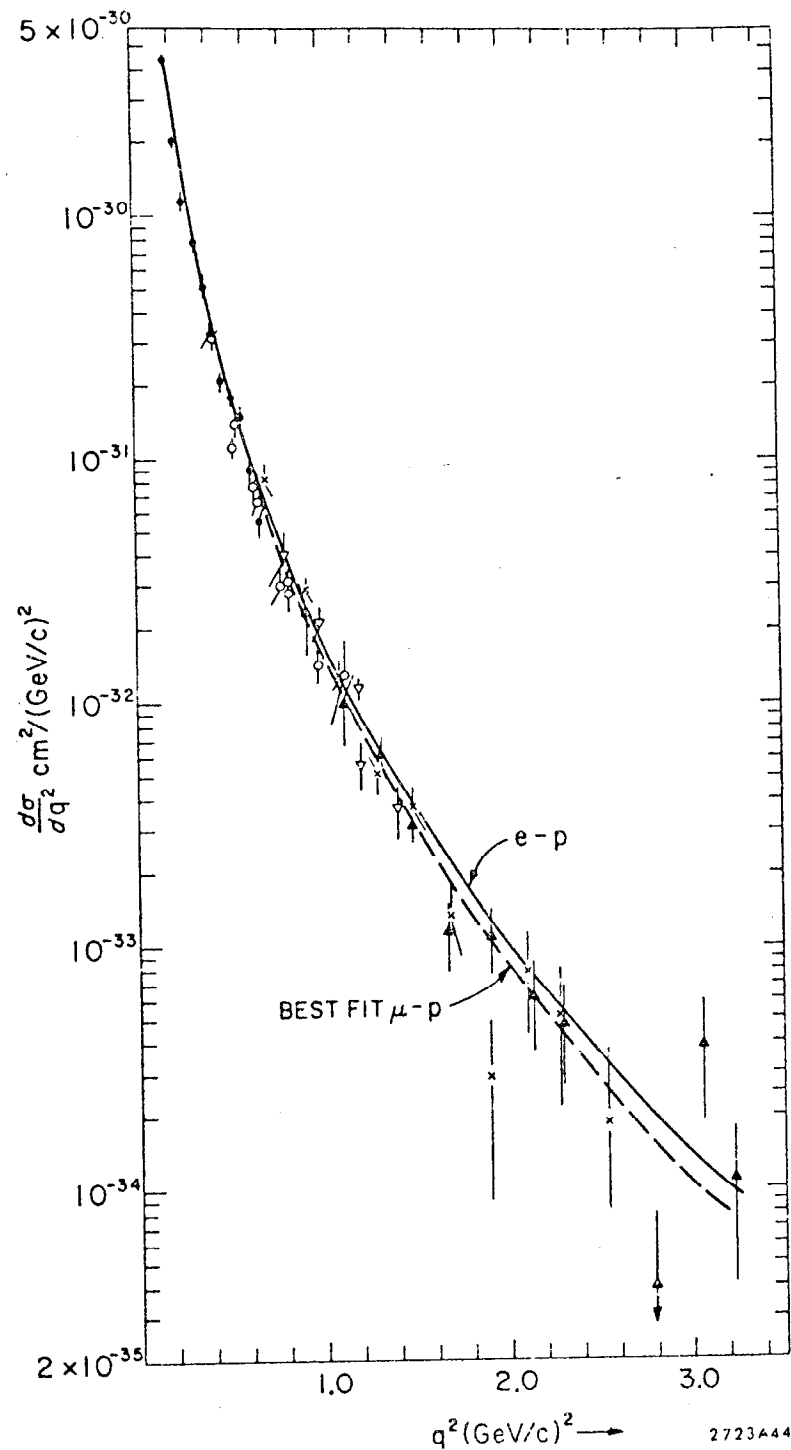
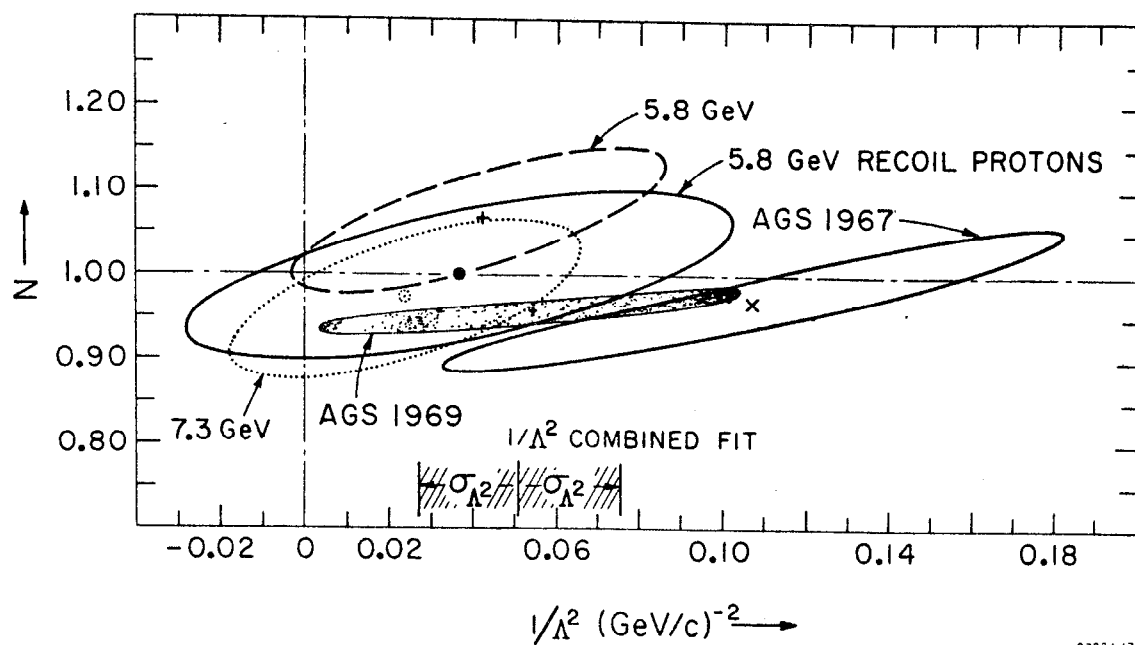


Fig. 20 The differential cross section  $d\sigma/dq^2$  for  $\mu-p$  elastic scattering. The solid curve represents the  $e-p$  data, and the dashed line is the best fit to the  $e-p$  function times a function  $r(q^2) \propto (1 + q^2/\Lambda^2)^{-2}$ .



2723A47

Fig. 21 One standard deviation contours for a fit to the results of 5 sets of  $\mu$ -p scattering data, with independent but constrained normalizations,  $N_i$ , and a common cut-off parameter  $1/\Lambda^2$ . The best fit<sup>i</sup> gives  $1/\Lambda^2 = 0.051 \pm 0.024$ .

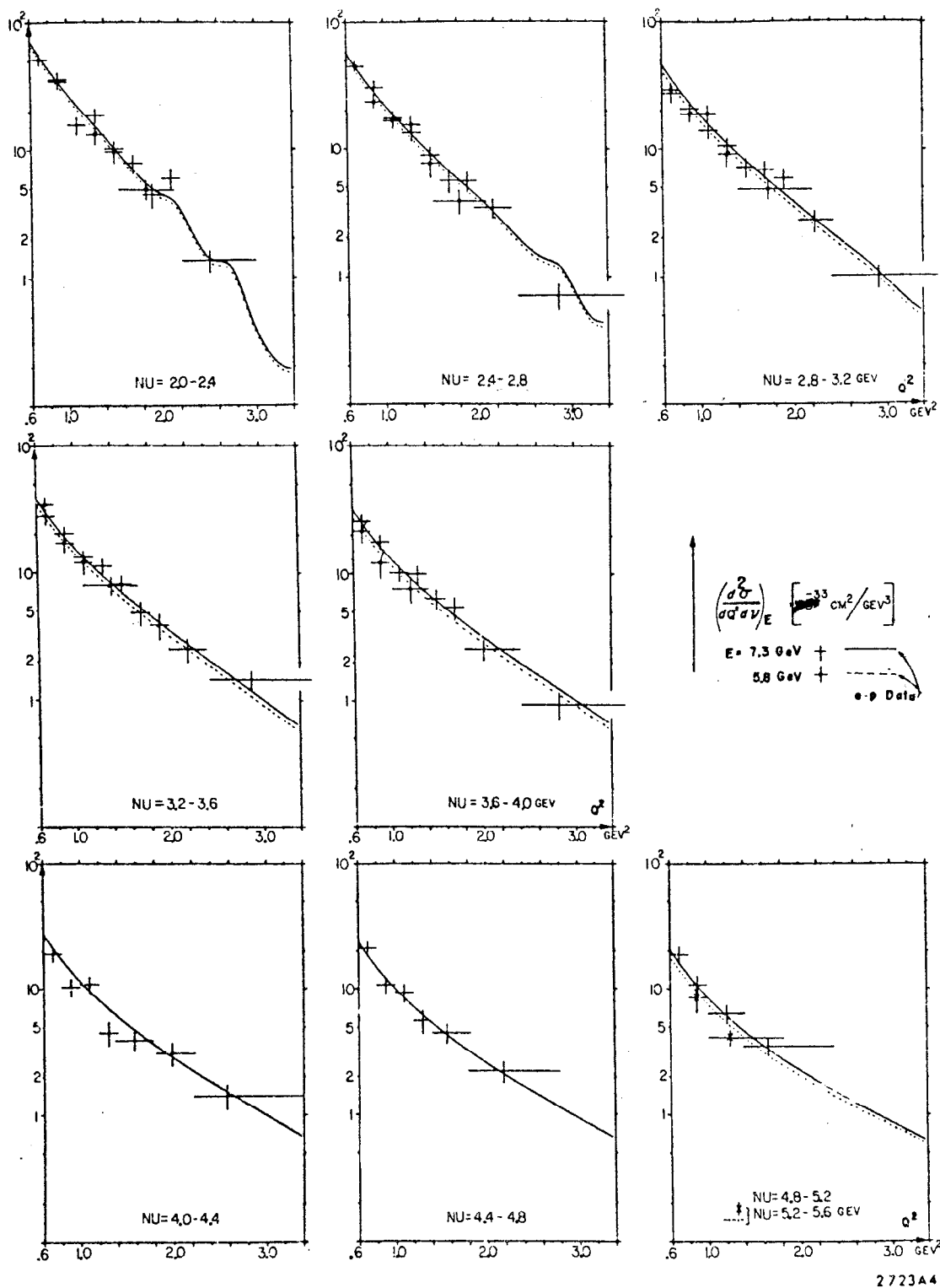


Fig. 22 Inelastic scattering cross section  $\frac{d^2\sigma}{dQ^2 dv}$  versus  $Q^2$  for fixed  $\nu$  intervals. The solid and dashed curves represent e-p data at  $E = 7.3 \text{ GeV}$  and  $5.8 \text{ GeV}$ .

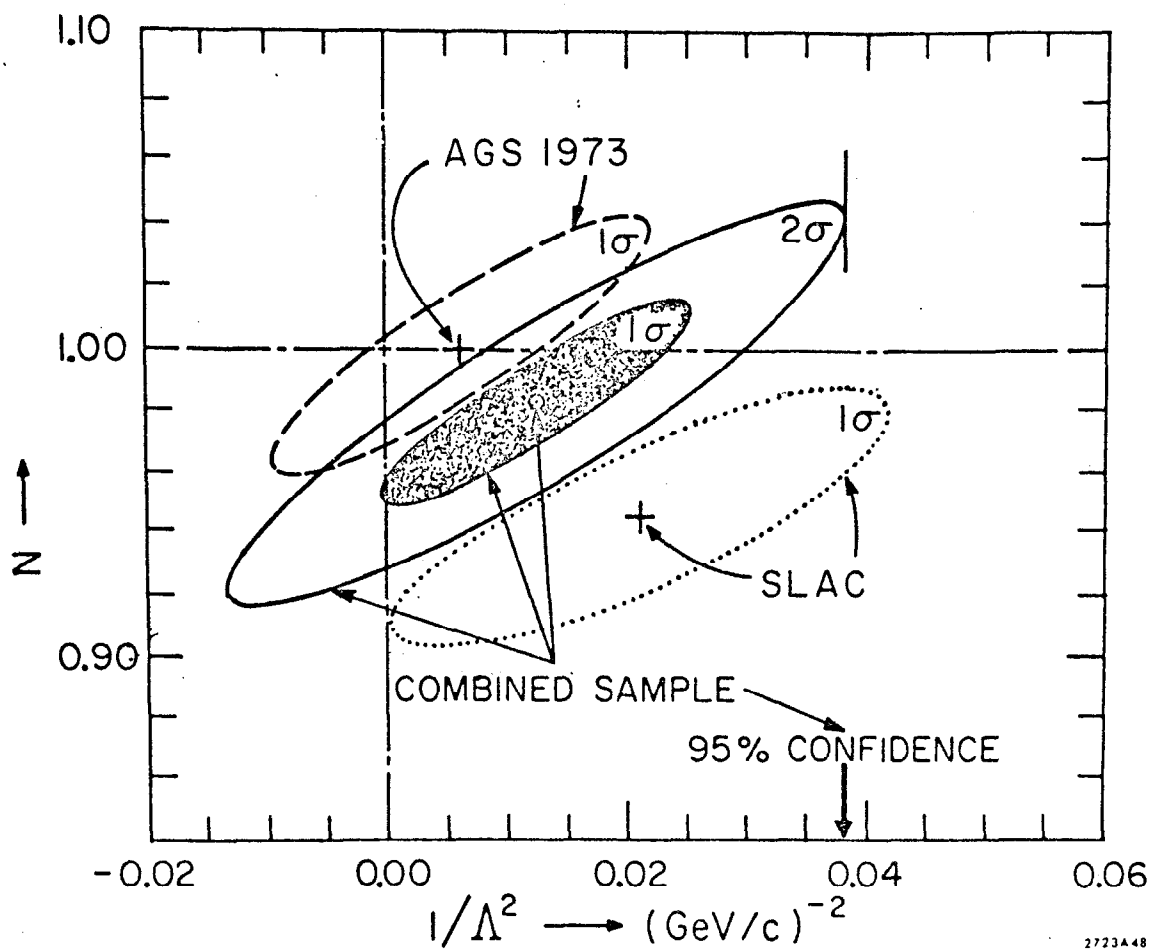


Fig. 23 A fit to the ratio  $\rho(q^2, \nu) = \nu W_2^{\mu} / \nu W_2^R$  of the form  $\rho(q^2, \nu) = N(1 + q^2/\Lambda^2)^{-2}$ . The best fit gives  $1/\Lambda^2 = 0.006 \pm 0.016$ , compatible with zero.

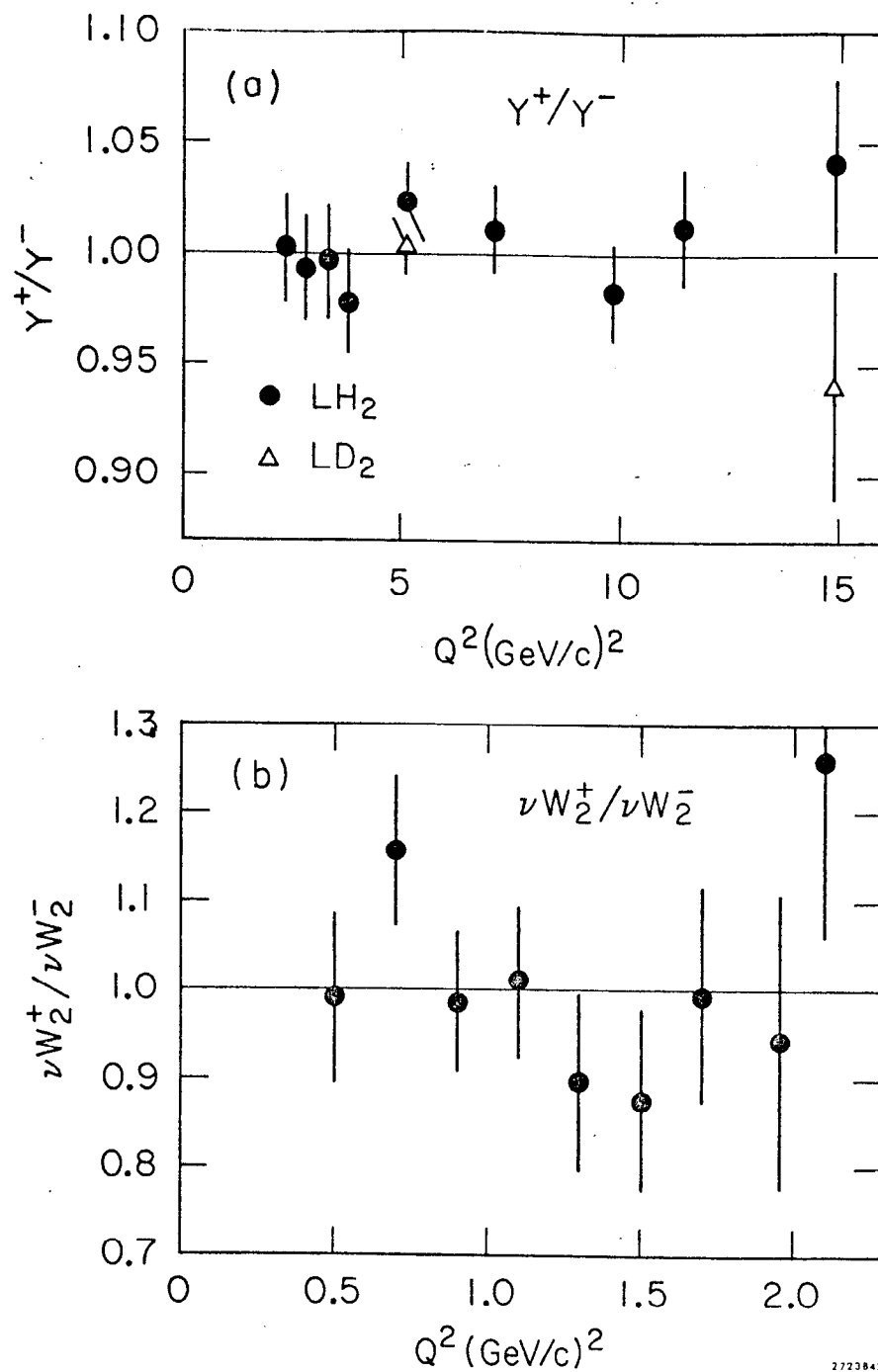


Fig. 24a) Ratio of yields  $Y^+/Y^-$ , of positron to electron inelastic scattering for values of  $Q^2$  up to 15(GeV/c) $^2$ .

Fig. 24b) Ratio of  $\nu W_2$  for  $\mu^+$  to that for  $\mu^-$  for  $Q^2$  up to 2.1(GeV/c) $^2$ . In both cases, the data are consistent with a ratio of unity.

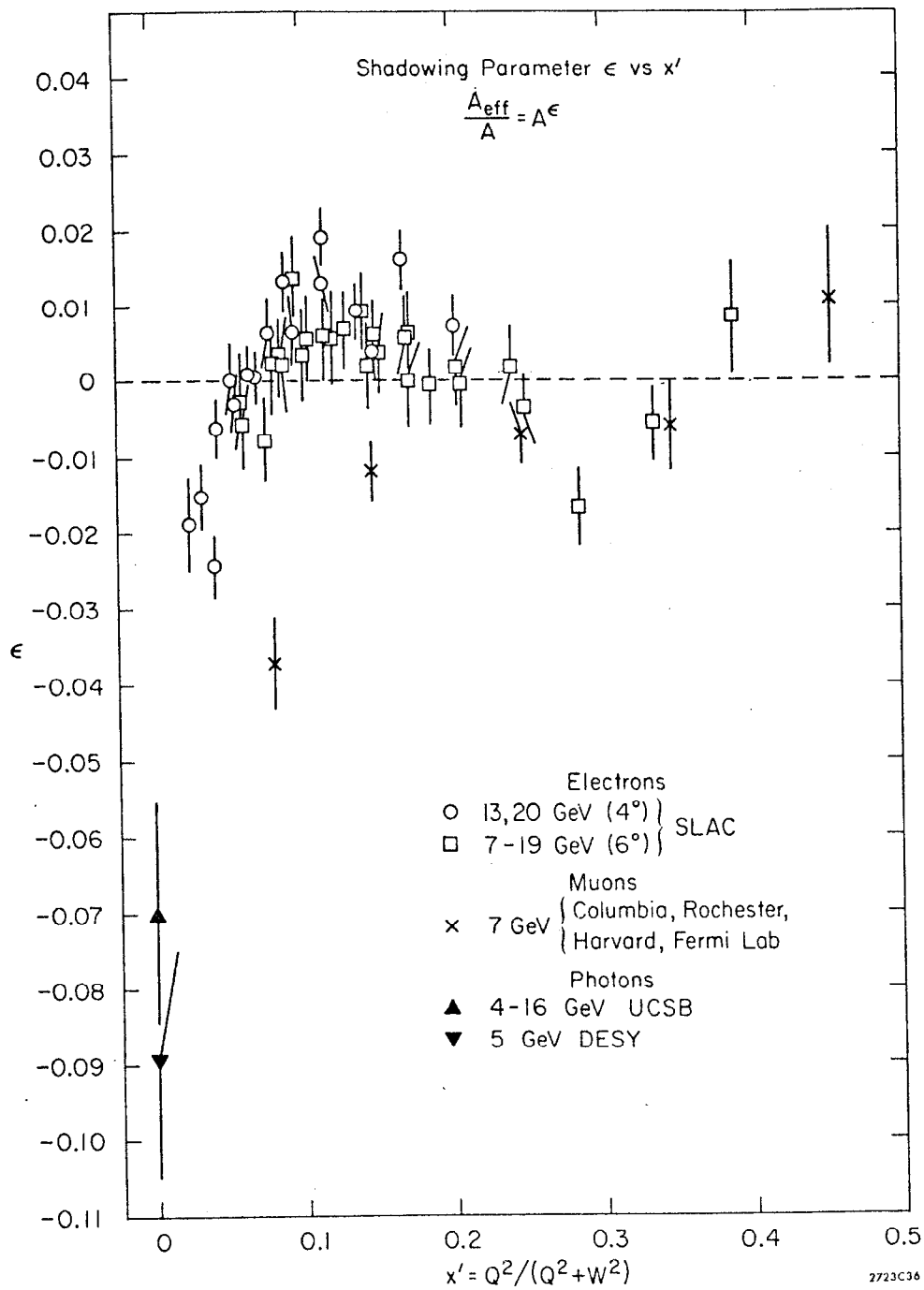


Fig. 25 The measured total cross section for a heavy nucleus divided by the cross section calculated for  $Z$  protons and  $A-Z$  neutrons is called  $A_{\text{eff}}/A$  which is then fit to  $A^\epsilon$ . Statistical errors are shown.

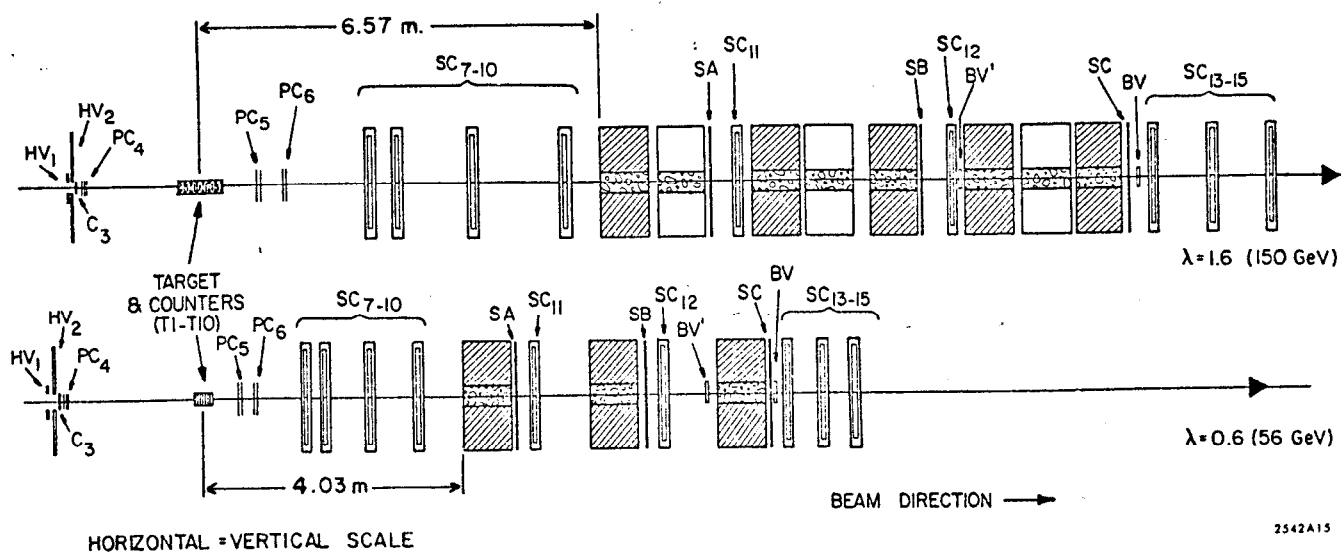


Fig. 26 Apparatus of the Cornell-Michigan-LBL experiment at FNAL. Shown are the configurations for 150 GeV and 56 GeV incident muons. The apparatus "scales" in the sense that particles of the same  $\omega$  go through the same part of the detector at both energies. Also, the number of iron magnets is adjusted so that the multiple scattering is the same in both cases.



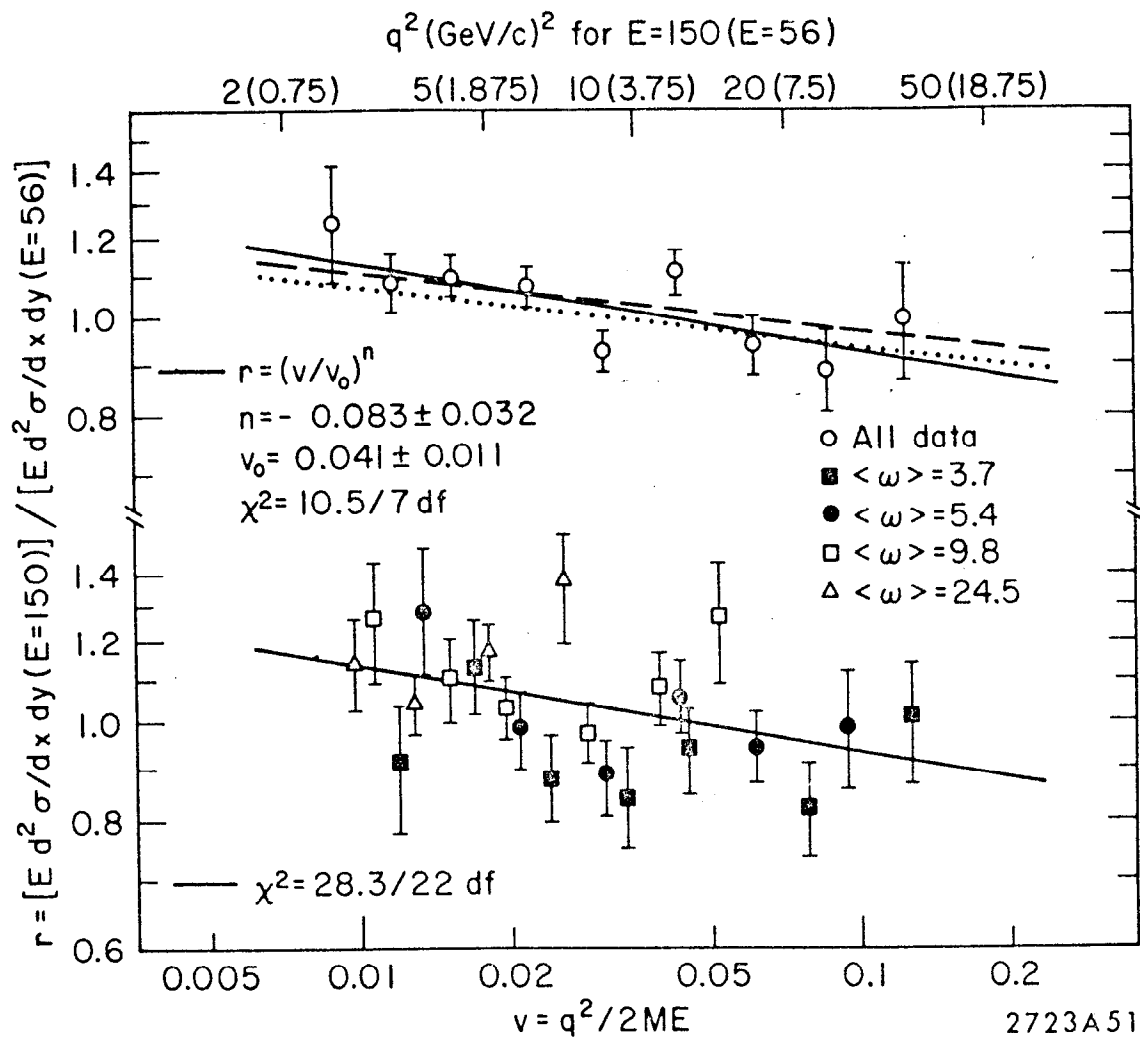


Fig. 27 The ratio,  $r$ , of the cross section at 150 GeV to that at 56 GeV vs.  $v$ . The solid lines are a power law fit to the data. The dashed line corresponds to increasing  $E'$  at 150 GeV by 1%, and the dotted line to assuming scaling in  $\omega$  rather than  $\omega'$  in the Monte Carlo.

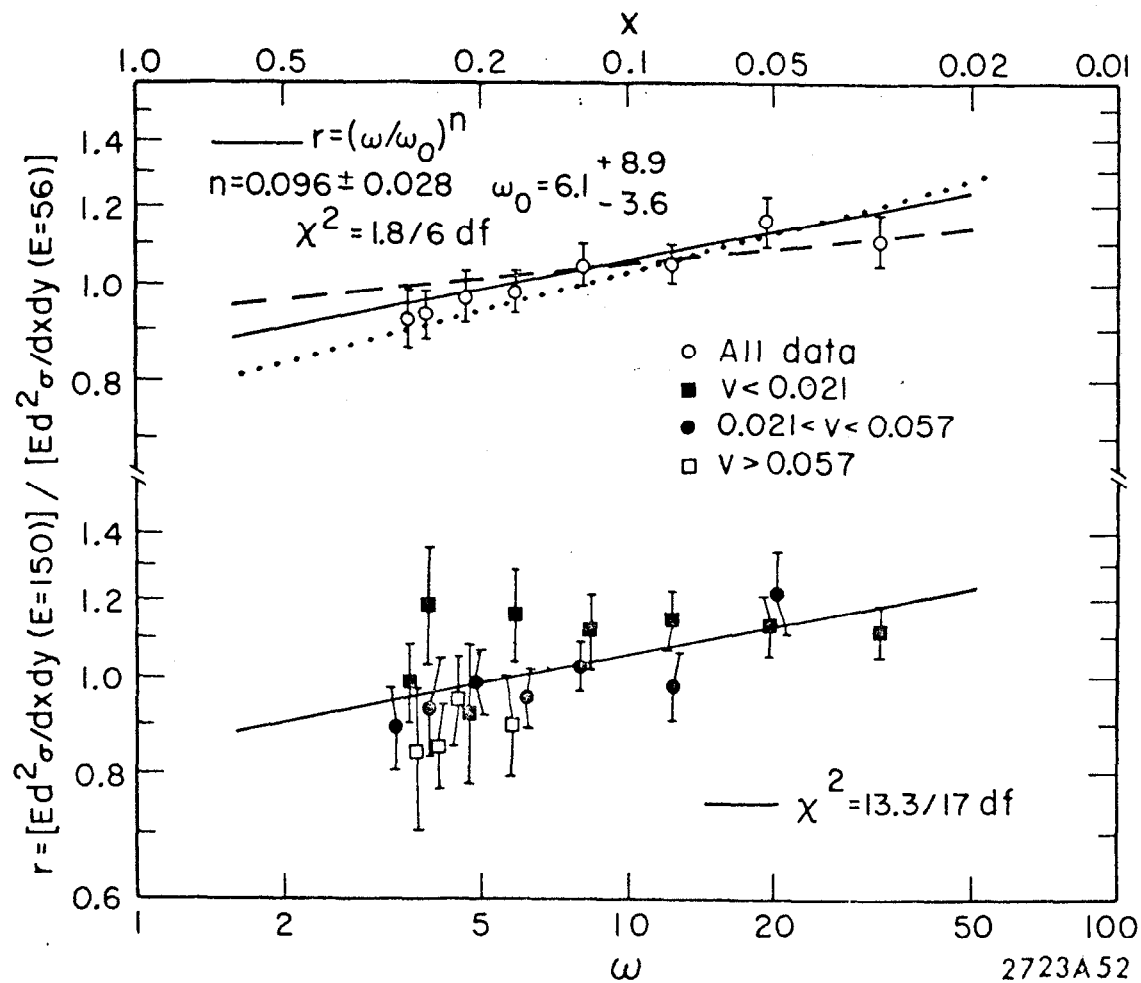


Fig. 28 The ratio,  $r$ , versus  $\omega$ . The meaning of the lines is the same as in the previous figure.

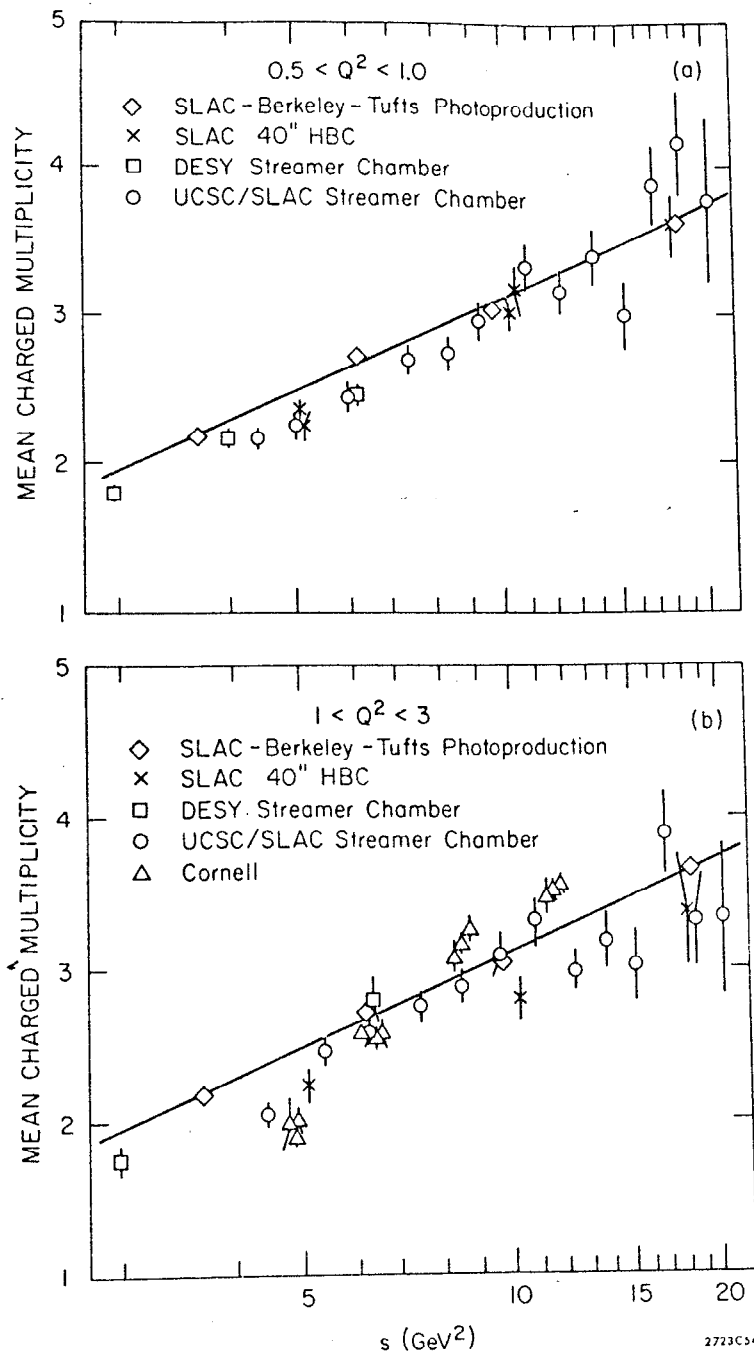


Fig. 29 The mean multiplicity for charged hadron production in inelastic  $e p$  and  $\mu p$  scattering is plotted versus  $s$  for two ranges of  $Q^2$ , .5 to 1.0 and 1 to 3  $\text{GeV}^2$ . Photoproduction data are also shown. The solid line is a fit of the form  $a + b \ln s$  to the photoproduction data.

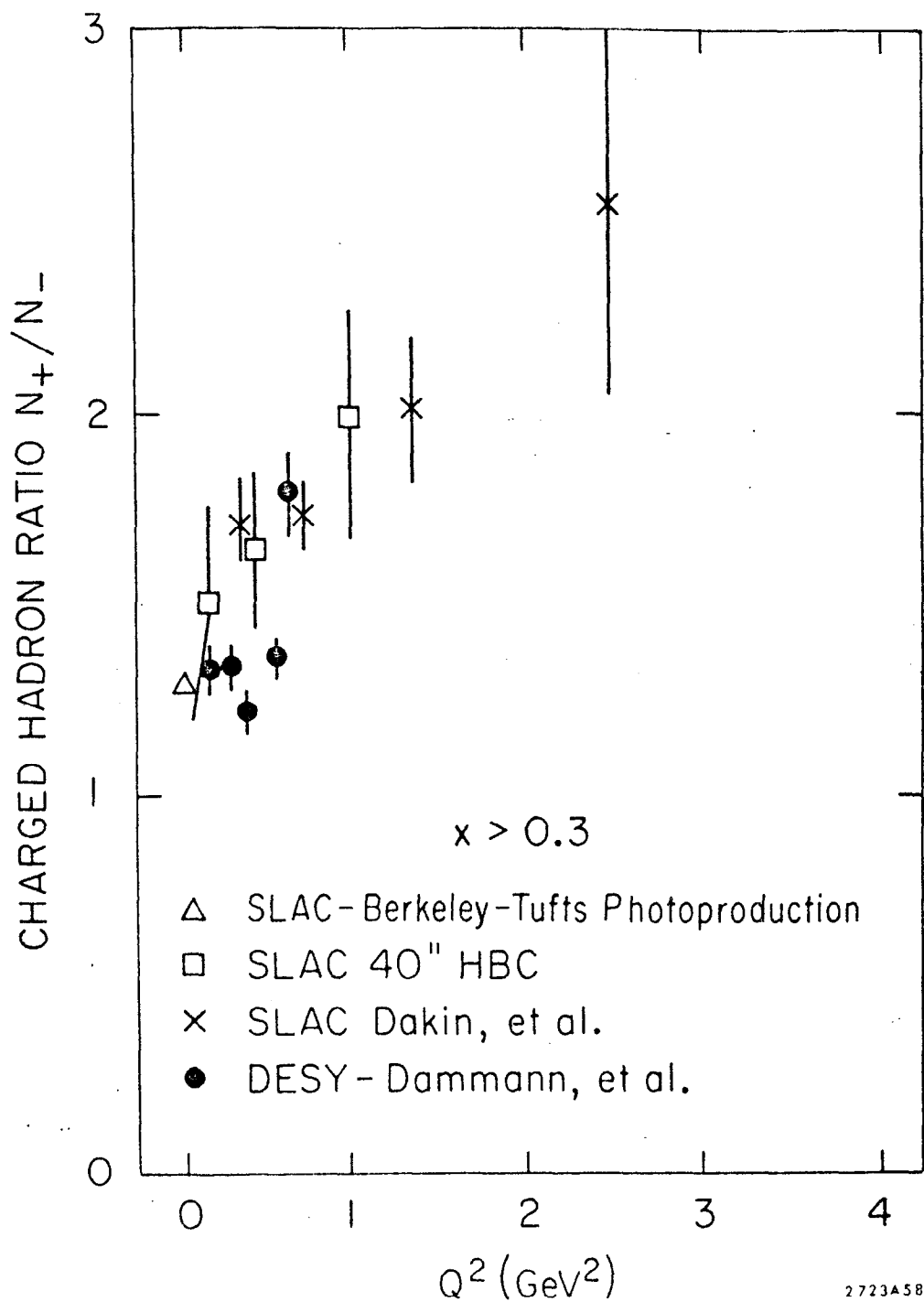


Fig. 30 The ratio of positively charged hadrons to negatively charged hadrons in the forward direction is plotted versus  $Q^2$  for  $x (=p_{\parallel}^*/p_{\text{max}}^*) > 0.3$ , for inelastic  $e p$  and  $\mu p$  scatterings. The value for photoproduction of hadrons is shown for comparison. The DESY values report the ratios  $\pi^+/\pi^-$ , while the other experiments include  $K$ 's and  $p$ 's as well.

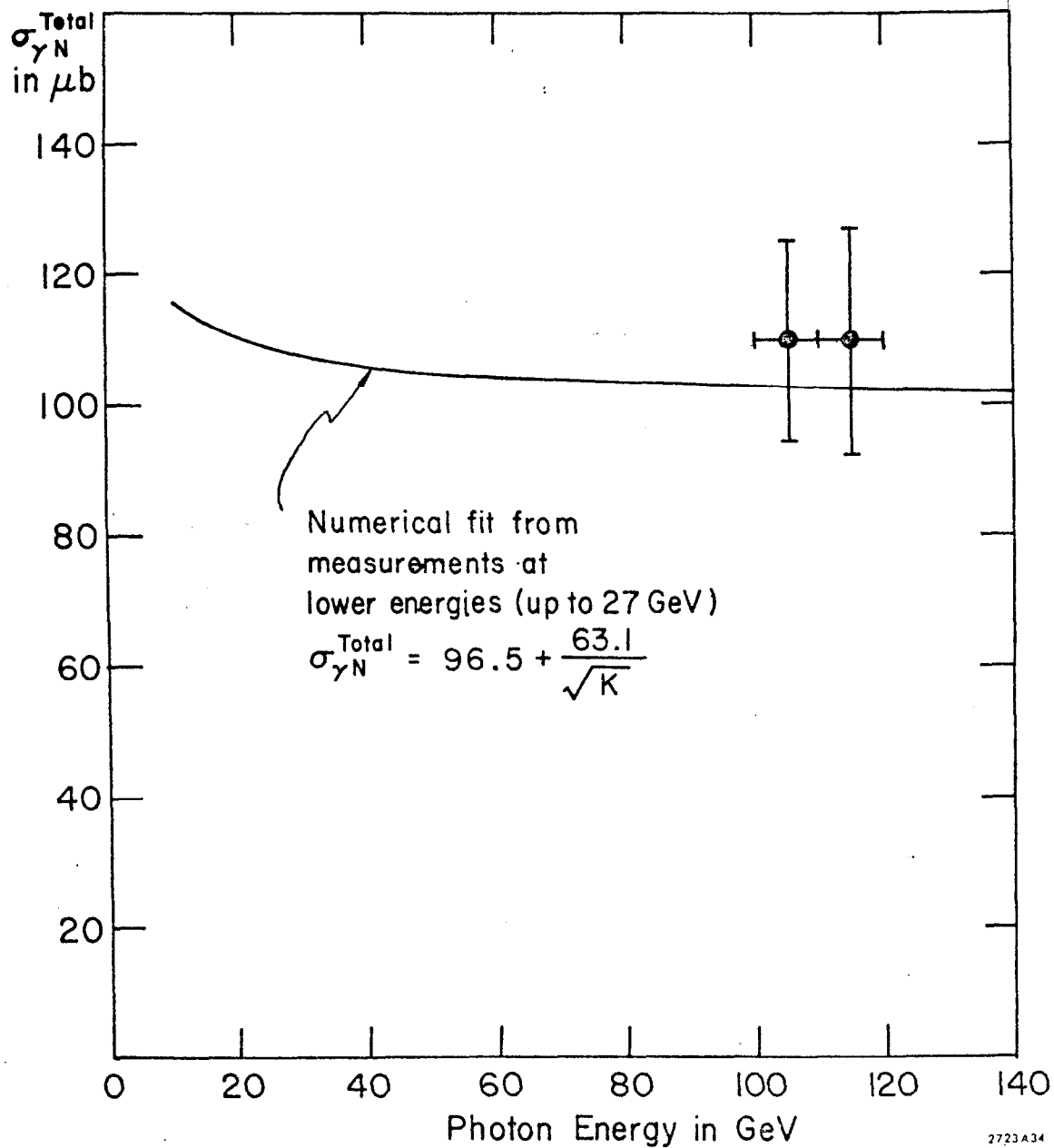


Fig. 31 The total photoabsorption cross section,  $\sigma_{\gamma N}^{\text{tot}}$  derived by extrapolation of inelastic muon scattering to  $Q^2 = 0$ . The equivalent energy is given by  $E_{\gamma} = K = (W^2 - M^2)/2M$